MATHEMATICAL APPROACH OF LIUTEX CORE LINE AND LIUTEX CORE TUBE FOR VORTEX STRUCTURE VISUALIZATION

by

DALAL ALMUTAIRI

Presented to the Faculty of the Graduate School of

The University of Texas at Arlington in Partial Fulfillment

of the Requirements

for the Degree of

DOCTOR OF PHILOSOPHY

THE UNIVERSITY OF TEXAS AT ARLINGTON

August 2021

ACKNOWLEDGEMENTS

Firstly, I want to give a heartfelt, special thanks to my dissertation chair, Dr. Chaoqun Liu, for his valuable time, prompt feedback, flexibility, expertise, constructive guidance, and encouragement during this dissertation work planning and development. I want to thank you, Dr. Liu, for allowing me to do my research under your guidance.

I wish to thank my dissertation committee Dr. Albert Tong, Dr. David Jorgensen, and Dr. Tuncay Aktosun, for their unlimited support, expertise, and encouraging words. Thanks for agreeing to serve my committee. I also would like to thank the Department of Mathematics at the University of Texas at Arlington, all faculty and staff, especially Dr. Hristo Kojouharov, for his academic support and guidance during my study. I had a wonderful experience with all the friendly people in the Department of Mathematics at UTA.

Dear Mom, Monerah Almutairi (1958 - 2013), I know that if you were among us today, you would be happy and proud of me as I am proud of you. I miss you a lot; may Allah be merciful to you. Dear Dad, Khalid Almutairi, I owe my deepest gratitude to your support, encouragement, prayers, and love. I cannot wait to see you soon!!

To my lovely husband, Dr. Nader Almutairi, this dissertation would not have been possible without your direct support. "Not All Heroes Wear Capes." That is true! Helping me to take care of our sweet children (Toleen, Fadah, Taim, and Lojain), working on your Ph.D. dissertation, and encouraging me to pursue my dreams, can only be done by heroes like you. I love you forever, and thank you for your everlasting patience.

I would like to express my sincere thanks to my colleagues in the Center for Numerical Simulation and Modeling (CNSM): Oscar Alvarez, Yifei Yu, Charles Nottage, Pushpa Shrestha, Vishwa Patel, and Aayush Bhattarai for giving me great experiences and the interesting discussions in our research sessions. I wish you all a prosperous future and continued success.

Moreover, I am thankful to my friends in UTA: Madhu Gupta, Asma Alghamdi, Vishwa Patel, Sundas (Sandy) Hussain, and other UTA friends. You made my experience in UTA enjoyable and wonderful, glad to have great friends like all of you.

ABSTRACT

MATHEMATICAL APPROACH OF LIUTEX CORE LINE AND LIUTEX CORE TUBE FOR VORTEX STRUCTURE VISUALIZATION

Dalal Almutairi, Ph.D.

The University of Texas at Arlington, 2021

Supervising Professor: Chaoqun Liu

During the past decades, many vortex identification methods have been published to present a clear definition and identification of the vortex. However, all these methods are failed to offer a unique identification method, and they also cannot answer the six essential issues for vortex identification methods, which are: 1) absolute strength, 2) relative strength, 3) rotational axis, 4) vortex core center location, 5) vortex core size, and 6) vortex boundary. In this work, two vortex identification methods, which are never affected by the threshold, will be proposed. Moreover, this study will address two critical questions: 1) Where is the rotational axis? 2)what is vortex core size? Liutex as a new physical quantity concept opens an era of turbulence research because Liutex introduces a scalar form and provides vector and tensor forms too. The Liutex vector represents the rotation part of fluid motion in isolation of the shear contamination.

Depending on a clear and reasonable mathematical approach, an exact Liutex core line and Liutex core tube algorithm will propose in this research. The results proved that the Liutex core line is the only vortex identification method unique so far. In addition, the result shows that

both the Liutex core line and Liutex core tube can expose the strength of the vortex, unlike the previous methods, which are iso-surface based. Since both methods, the Liutex core line and Liutex core tube, have been extracted by Liutex lines, they both get another advantage showing the vortex direction. Even though the Liutex core tube is not a unique vortex identification method, comparing the Liutex core tube and the iso-surface-based methods displays the superiority of the Liutex core tube in showing the strong and weak spots of the vortex structure clearly. The proposed algorithms have been implemented on the Direct Numerical Simulation (DNSUTA) data of flow transition in boundary layers, which is pre-processed and validated by researchers from UTA and NASA Langley.

TABLE OF CONTENTS

LIST OF ILLUSTRATIONS

CHAPTER 1

INTRODUCTION

In fluid mechanics, the vortex is the essential part of formulating the turbulent flow where the turbulent flows have uncountable vortices of different sizes and strengths. Therefore, presenting an accurate and precise definition of vortices is extremely important. However, visualizing and defining vortices is an open challenge in fluid mechanics decades ago, which led to the development of three different generations of vortex identification methods. For this reason, turbulence research has faced significant confusion and false impression.

The vortex identification methods are classified as [27] the vorticity-based vortex identification methods and eigenvalue-based vortex identification methods as the first and the second generation, respectively. The third generation of the vortex identification methods has been introduced as Omega, Liutex (previously known as Rortex), Omega-Liutex methods. Several vortex identification methods have been proposed to produce an accepted mathematical definition in the last three decades, which all faced limitations, disadvantages, and failure to do so for many reasons. Based on the vorticity filaments and tubes, the first generation shows weakness in the near-wall turbulence; it is still used in many textbooks and research papers [35,40]. Q, Δ, λ_{ci}, and λ_2 are labeled as the second generation methods, which all can be considered rotational strength and iso-surfaces. That means the visualization of the vortical structures in flow fields depends on the thresholds that are selected by the users [13]. In 2014, Prof. Chaoqun Liu; is currently the Tenured and Distinguished Professor at UTA, has formed a research team at the University of Texas at Arlington focused on vortex and turbulence research. The team's great submitted effort has yielded to the Omega method, which considers the vortex a

connected region where the vorticity transcends the deformation. In 2018, Dr. Liu and his team had proposed the Liutex method, a mathematical tool-up of vortex identification methods that rigid the local rotation part of the fluid motion. Then in 2019, Omega-Liutex, which associates the benefit of both Liutex and Omega methods has introduced. Omega, Liutex, and Omega-Liutex are classified as the third generation of vortex identification methods [27]. The third-generation methods can address six main issues related to the vortex identification methods, which are: 1) absolute strength, 2) relative strength, 3) rotational axis, 4) vortex core center location, 5) vortex core size, and 6) vortex boundary [41].

In this study, the main contribution is proposed an exact algorithm, dependent on clear and reasonable mathematical explanations, to answer two of the vortex definition and identification methods issues using the Omega-Liutex method as follows. 1) Finding the rotational axis (Liutex core line) after determining the core point's location. 2) Defining the vortex core size by finding the vortex core tube. The vortex core line's literature reviews and the vortex core tube will be described in the following sections.

1.1 Vortex core line identification methods

1.1.1 The first and second generations based definition of vortex core line (rotation axis)

Vortex core line (rotation axis) identification methods show up the rotation vortices center using some algorithms. Sujudi and Haimes [38] presented their approach for detecting the center of rotation in individual cells based on the old-fashioned generation of vortex identification methods. Even though this method fails for the complex vortices, Roth [36] modified it in parallel vector operators to introduce a simplification of the vortex center. Roth combines the methods of Sujudi and Haimes [38], Levy et al. [26], Banks and Singer [5], Kida and Miura [23],

and Strawn et al. [37] into one algorithm implementation. However, since all of the previous methods are based on the velocity or the pressure, the first and second generations of vortex identification face several disadvantages. See chapter 2 for more details.

1.1.2 The Liutex based definition of vortex core line (rotation axis)

Since Liutex gives an extending meaning to include the direction beside the magnitude, as stated in chapter 2, the Liutex lines, which integrate the Liutex vector can find, are continuous in the vortex region uniquely. That has been applied to expound the skeleton of the hairpin vortices in [13, 33]. Gao et al.[14] introduce the manual method to extract the Liutex core line by combining the Liutex lines and the Liutex magnitude gradient lines. The rotation axis line concept was presented in [14] as the concentration of Liutex magnitude gradient lines. The concentration lines intersect on the plane perpendicular to the vortex rotation axis line via the local Liutex maxima point. This line is a Liutex vector that is only aligned with the direction of the Liutex magnitude gradient.

Although Xu et al.[43] had presented an automatic method for finding the Liutex core line by the end of 2019, but the algorithm that was used is unclear for some somehow. According to the original paper, the vortex core line automated process was developed by fully implementing the definition of Liutex magnitude and $\nabla R \times \vec{r} = 0$ into a computer program. However, applying only this condition does not lead to a unique Liutex core line in practice, especially in severely curved vortices. In chapter 3, more explanations in detail will be provided.

1.2 Vortex core tube identification methods: overview of the previous work

1.2.1 The first and second generations based definition of vortex core tube

In 1858, Helmholtz [18] had introduced the concept of vortex tube and vortex filament for the first time. From on Helmholtz theorems, *vortex filament* can be defined as an imaginary curve within a rotating fluid surrounding its core center formulated by the vortex lines via all the points of this curve. There is a general belief based on what Helmholtz presented: vortices can be contained in small vorticity tubes. Moreover, the vortex strength is the magnitude of the vorticity; that is, the velocity curl. Even though these methods, which are based on the first generation, are failed, the vortex filament is still used as a visualization turbulence tool in many studies such as Hanninen et al.[17] in 2014.

In 2016, Dong et al. [11] have used two different methods from two different generations: λ_2- method and vortex filaments method of the second generation and the first generation, respectively, to visualize the vortex structure turbulence. However, since both generations are faced several disadvantages, as will be stated in chapter 2, this mixture will have similar shortages.

1.2.2 The Liutex based definition of vortex core tube

Since the vortex core tube can be stated as the central area where fluid has a rotation, the vortex core line is the cornerstone of creating the vortex core tube. In other words, the vortex core tube depends on the vortex core line accuracy that is used for tubing construction.

In 2021, Alvarez et al. [2] have proposed a manual method to visualize the Liutex core tube using the Liutex core line. First, Gao's manual method has been used to extract the Liutex core line, introduced in [14]. Then, the Liutex core tube magnitude vector is defined concerning

an arbitrary percentage around the core line, resulting in the vortex core tube. See chapter 4 for more details. Although Alvarez et al. had presented a successful manual method for finding the Liutex core tube, creating Liutex core tube for complex and severely curved vortices manually seems impossible in this manual way.

1.3 The DNSUTA of flow transition in boundary layers

In 2009, the UTA team developed the DNSUTA; Direct Numerical Simulation (DNS) of flow transition in boundary layers, which was released by prof. Chaoqun Liu. UTA and NASA Langley researchers have validated the DNSUTA in [44, 29, 6]. Furthermore, the results of DNSUTA were also compared and other's DNS results where the DNSUTA shows a remarkable consistency over which means it is correct and accurate in [4,25].

According to Yan, Y. et al. [44] and Liu, C. et al. [29], the grid plane is $1920 \times 128 \times 241$, which represents the number of grids in streamwise (X) direction, spanwise (Y) direction, and wall-normal (Z) direction respectively, see Figure 1.1 and Figure 1.2.

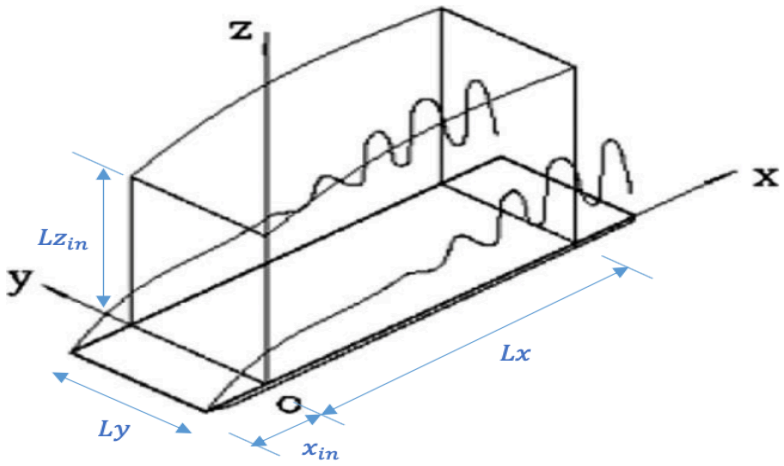

Figure 1.1.The DNS computation domain

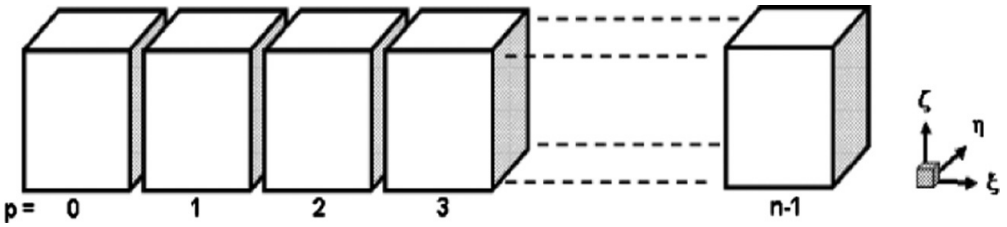

Figure 1.2. The DNS domain decomposition with respect to the streamwise (X) direction

The grid is uniform in the streamwise (X) and spanwise (Y) directions, but it is stretched in the normal direction (Z). The flow parameters are presented in Table 1.1; see [44, 29] for further details.

Table 1.1: The DNS parameters definitions and values

The parameter	**The value**	**The detention of the parameter**
M_∞	0.5	Mach number
Re	1000	Reynolds number
x_{in}	$300.79\delta_{in}$	distance between leading edge of flat plate and upstream boundary of computational domain
Lx	$798.03\delta_{in}$	length of computational domain along x direction
Ly	$22\delta_{in}$	length of computational domain along y direction
Lz_{in}	$40\delta_{in}$	height at inflow boundary
T_w	$273.15K$	wall temperature
T_∞	$273.15K$	free stream temperature

Where δ_{in} denotes the inflow displacement thickness. In this dissertation, The DNSUTA of flow transition in boundary layers is used for the test cases.

This dissertation is organized as follows. In Chapter 2, an overview of the first and second generations of vortex identification methods is given. The third generation of vortex identification methods is discussed in more detail. The modified Liutex-Omega method, which is used to extract the local maximum points in this work, is explained by introducing the reasons for using it. In Chapter 3, the Liutex core line is determined uniquely by an algorithm that depends on mathematical reasonable based. The core center points are selected first. Then Liutex line plotted through them after exclude the fake points. In Chapter 4, an algorithm to create a Liutex core tube, depending on the Liutex core line found in chapter 3, is proposed. The core tube that is found can show the structure size of the vortex. In Chapter 5, the study's conclusions are shown by demonstrating a summary of the results for the whole research. At the end of this chapter, some prospective studies have been provided based on this research.

CHAPTER 2

VORTEX IDENTIFICATION METHODS: OVERVIEW OF THREE GENERATIONS

For providing a clear definition of the vortex, there are three different generations classified as vortex identification methods. In this chapter, the first and second generations will be introduced in the beginning. The third-generation includes the Omega method, Liutex method, Liutex-Omega method will be described in the second section. Since this dissertation's primary methods are the Liutex and Liutex-Omega methods, the researcher will explain them in detail. The three generations of vortex identification methods will be discussed as follows.

2.1 The first generation: vorticity-based of vortex identification methods

In 1858, Helmholtz proposed vorticity filament and tube concepts. Based on his definition, there are three vortex theorems, which are considered as principles of vorticity dynamics, are obtained in [27] as the following: (1) The vortex filament strength is constant along its length, (2) In the fluid, the vortex filament never ends, so it has to form a closed path or prolong to the fluid boundaries, and (3) If there are no external rotational forces, a fluid that is at first irrotational remains irrotational. Even though there are some researchers have been applied vorticity filament and tube concepts introduced by Helmholtz to identify the vortex structures [24,17], the laminar boundary layer exemplifies the failure of this method where the average shear force created by the no-slip wall is strong while there are no rotation motions near-wall regions. In 2017, Wang et al. [40] show that for a transitional flow over a flat plate in the boundary layer's near-wall region, the local vorticity vector can be misrepresented from the vortex structure. Also, the vortex may show up in a space where vorticity is smaller than the

surrounding area so that the vorticity is larger than the vorticity inside the vortex. See Figure 2.1 and Figure 2.2.

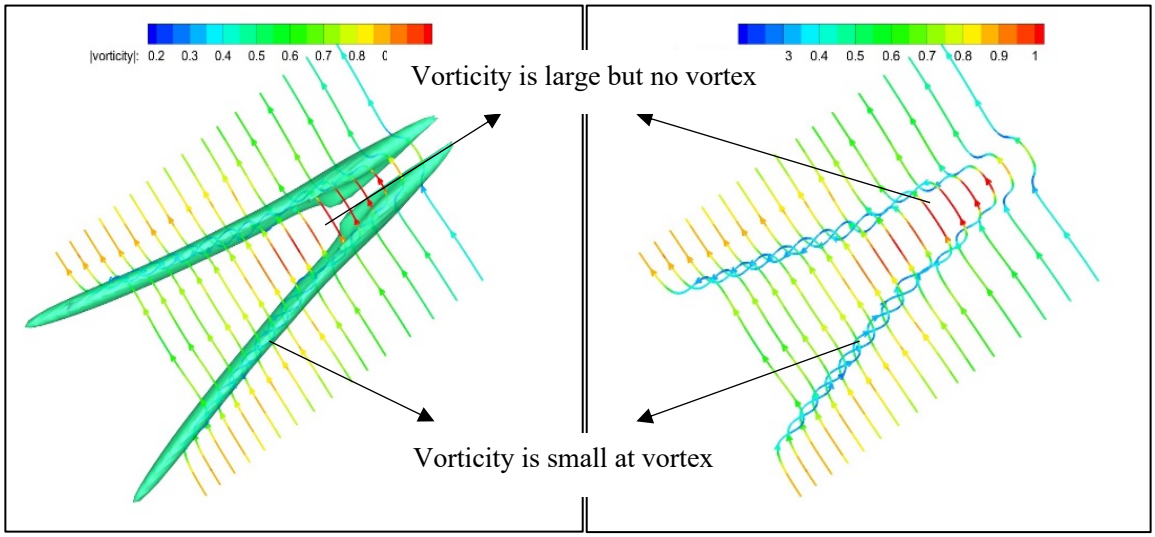

a) With iso-surface b) Without iso-surface

Figure 2.1: Vorticity line is not aligned with the legs of $\Lambda -$ vortex and Vorticity is smaller than surrounding of $\Lambda -$ vortex

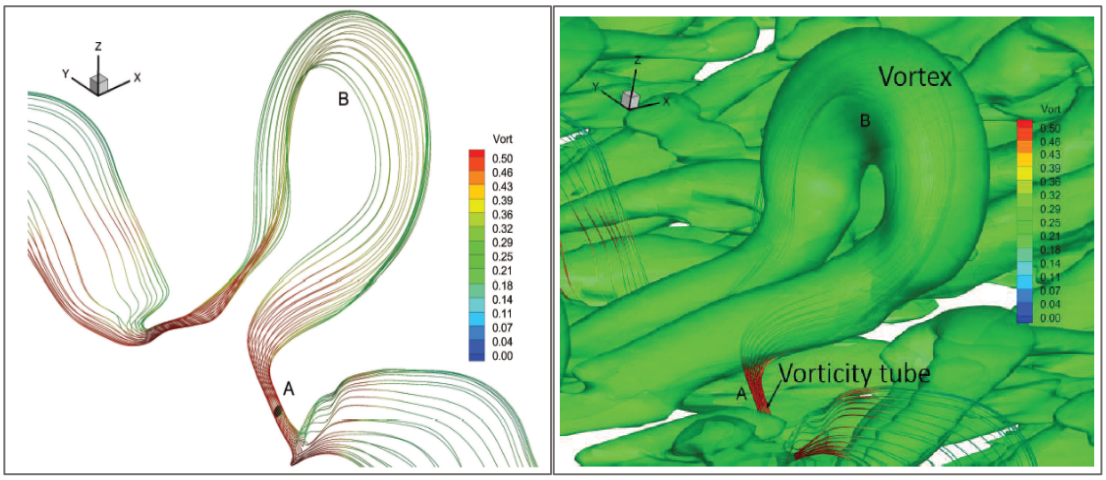

a) Without iso-surface b) With iso-surface

Figure 2.2: Vorticity tube and vortex tube are not aligned and not correlated in vortex rings

Liu et al. [30] have made several sensible arguments that refute allegations that Helmholtz's vortex definition and three theorems are the foundation of modern vortex (vorticity) dynamics. Since the vortex cannot be ended inside the flow field, as Helmholtz stated, how does the vortex breakdown generate turbulence? However, a vortex can break down, which means the vortex is not vorticity tubes as assumed. By correlation analysis (fluid rotation), it is founded that there is no correlation between vortex and vorticity in general, which led us to say, "vortex is not vorticity."

2.2 The second generation: eigenvalue-based vortex identification methods

The second generation of vortex identification methods is classified as Eulerian velocity-gradient-based criteria. These criteria are common to use in research and engineering since they are Galilean invariant. Consider the velocity gradient decomposition; Cauchy-Stoke decomposition, like the following:

$$\nabla\vec{v} = \frac{1}{2}(\nabla\vec{v} + \nabla\vec{v}^T) + \frac{1}{2}(\nabla\vec{v} - \nabla\vec{v}^T) = \boldsymbol{A} + \boldsymbol{B} \tag{2.1}$$

where $\boldsymbol{A}$ and $\boldsymbol{B}$ represent symmetry and anti-symmetry parts, respectively. Q-criterion, Δ-criterion, λ_{ci}-criterion and λ_2-criterion are four eigenvalue-based criteria. Since the Q and λ_2 criteria are the most popular used methods, they will be briefly addressed.

2.2.1 $\boldsymbol{Q}$-criterion:

In 1988, Hunt et al.[20] proposed the Q-criterion as a vortex identification method. Q method can be defined as a measure of the local rotation rate over the strain rate and positive second invariant, which is expressed the balance between vorticity magnitude and shear strain rate. Q can be inferred as:

$$Q = \frac{1}{2}(\|\boldsymbol{B}\|_F^2 - \|\boldsymbol{A}\|_F^2) \tag{2.2}$$

where $\|\cdot\|_F^2$ represents the Frobenius norm. $\boldsymbol{A}$ and $\boldsymbol{B}$ the symmetric and antisymmetric parts of the velocity gradient tensor respectively, expressed as follows:

$$\boldsymbol{A} = \frac{1}{2}(\nabla\vec{v} + \nabla\vec{v}^{\mathrm{T}}) = \begin{bmatrix} \frac{\partial u}{\partial x} & \frac{1}{2}\left(\frac{\partial u}{\partial y} + \frac{\partial v}{\partial x}\right) & \frac{1}{2}\left(\frac{\partial u}{\partial z} + \frac{\partial w}{\partial x}\right) \\ \frac{1}{2}\left(\frac{\partial v}{\partial x} + \frac{\partial u}{\partial y}\right) & \frac{\partial v}{\partial y} & \frac{1}{2}\left(\frac{\partial v}{\partial z} + \frac{\partial w}{\partial y}\right) \\ \frac{1}{2}\left(\frac{\partial w}{\partial x} + \frac{\partial u}{\partial z}\right) & \frac{1}{2}\left(\frac{\partial w}{\partial y} + \frac{\partial v}{\partial z}\right) & \frac{\partial w}{\partial z} \end{bmatrix} \text{ and} \tag{2.3}$$

$$\boldsymbol{B} = \frac{1}{2}(\nabla\vec{v} - \nabla\vec{v}^{\mathrm{T}}) = \begin{bmatrix} 0 & \frac{1}{2}\left(\frac{\partial u}{\partial y} - \frac{\partial v}{\partial x}\right) & \frac{1}{2}\left(\frac{\partial u}{\partial z} - \frac{\partial w}{\partial x}\right) \\ \frac{1}{2}\left(\frac{\partial v}{\partial x} - \frac{\partial u}{\partial y}\right) & 0 & \frac{1}{2}\left(\frac{\partial v}{\partial z} - \frac{\partial w}{\partial y}\right) \\ \frac{1}{2}\left(\frac{\partial w}{\partial x} - \frac{\partial u}{\partial z}\right) & \frac{1}{2}\left(\frac{\partial w}{\partial y} - \frac{\partial v}{\partial z}\right) & 0 \end{bmatrix} \tag{2.4}$$

After applying (2.3) and (2.4) in (2.2), Q can be rewritten as the following:

$$Q = \frac{1}{2}(\|\boldsymbol{B}\|_F^2 - \|\boldsymbol{A}\|_F^2) \tag{2.5}$$

$$= -\frac{1}{2}\left[\left(\frac{\partial u}{\partial x}\right)^2 + \left(\frac{\partial v}{\partial y}\right)^2 + \left(\frac{\partial w}{\partial z}\right)^2 + 2\frac{\partial u}{\partial y}\frac{\partial v}{\partial x} + 2\frac{\partial u}{\partial z}\frac{\partial w}{\partial x} + 2\frac{\partial v}{\partial z}\frac{\partial w}{\partial y}\right]$$

2.2.2 λ_2 criterion :

One of the most common eigenvalue-based vortex identification methods is λ_2- criterion, which had been proposed by Jeong & Hussain [21] in 1995. Let λ_1, λ_2, and λ_3 are the eigenvalues of the symmetric tensor $\boldsymbol{A}^2 + \boldsymbol{B}^2$; Jeong & Hussain define the vortex core as a connected region if the eigenvalues are ordered as $\lambda_1 \geq \lambda_2 \geq \lambda_3$; which is equivalent to $\lambda_2 < 0$. In general, λ_2 can not be expressed in terms of the eigenvalues of the velocity gradient tensor. The only particular case to do so is when the eigenvectors are orthonormal.

Table 2.1: Eigenvalue-Based Vortex Identification Methods

Name	**Authors**	**Year**
$\boldsymbol{Q}$ **criterion**[20]	Hunt, Wray, Moin	1988
Δ **criterion**[7]	Chong, Perry	1990
$\boldsymbol{\lambda_2}$ **criterion**[21]	Jeong, Hussain	1995
$\boldsymbol{\lambda_{ci}}$ **criterion**[45]	Zhou, Adrian, Balachandar	1999

2.2.3 The limitations of the eigenvalue-based vortex identification methods

In 2021, Liu et al. [31] highlight the eigenvalue-based vortex identification methods disadvantages in three main points: threshold, rotation direction, and strength of vortex. The previous eigenvalue-based criteria require thresholds that the user specifies. The threshold is a sensitive issue for identifying the vortical structure where different thresholds will indicate different vortical structures. Figure 2.3.a) shows a vortex breakdown for applying a large threshold for the λ_2 criterion, while Figure 2.3.b) shows a connected vortex when a small threshold is used. So the question here is: what is the appropriate threshold? Although no one knows whether the specified threshold is proper or improper, finding the appropriate threshold is related to empirical, sensitive, time step-related, and hard to adjust case by case and even time step by time step. Moreover, these vortex identification methods give iso-surface, which is contaminated by shear and stretch in different degrees, and they provide no information about the rotation axis and the direction of the vortex.

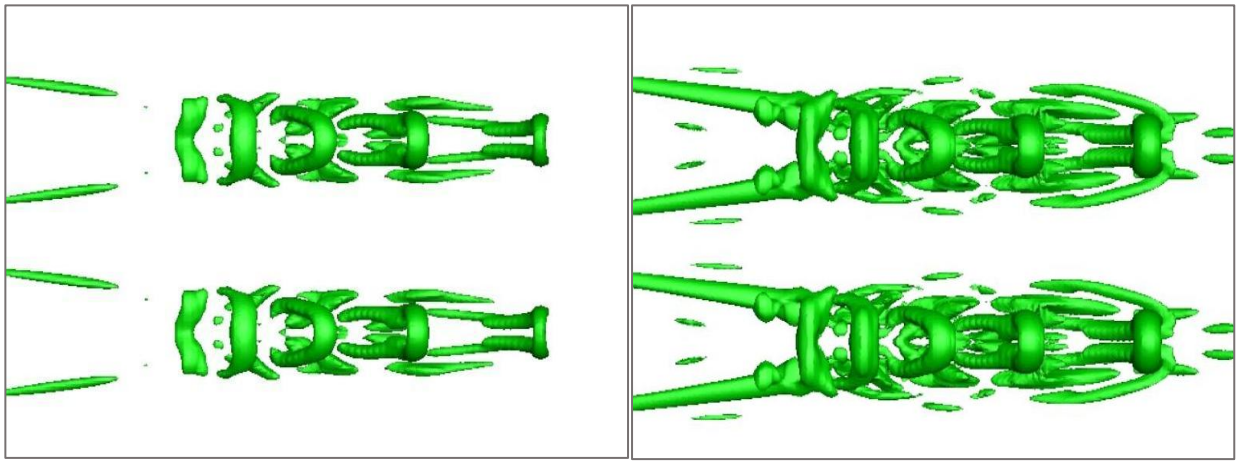

a) $\lambda_2 = -0.017$ b) $\lambda_2 = -0.003$

Figure 2.3: A large threshold of $\lambda_2 = -0.017$ leads to vortex breakdown in a) while a small threshold of $\lambda_2 = -0.003$ leads to data connected (no vortex breakdown) in b)

2.3 The Third Generation of Vortex Identification Methods: Omega, Liutex, Liutex-Omega, and Modified Liutex-Omega methods

Professor Chaoqun Liu, Distinguished Professor and Director of the Center for Numerical Simulation and Modeling, and his team at the University of Texas at Arlington initiated developing new vortex identification methods that can outdo the shortcomings of the first and second-generation identification methods in 2014. These serious researches produced the third generation of vortex identification methods based on the Omega and Liutex methods[30].

2.3.1 Omega vortex identification method

Liu et al. [32] had proposed the Omega method based on the physical meaning, which is vortex is the area that vorticity exceeded the deformation in 2016. So, it is sensible to consider the ratio of vorticity and deformation when setting a definition of the vortex. According to the

original paper [32], the Omega method is defined as a ratio of vorticity tensor norm squared over the sum of vorticity tensor norm squared and deformation tensor norm squared:

$$\Omega = \frac{\|\boldsymbol{B}\|_F^2}{\|\boldsymbol{A}\|_F^2+\|\boldsymbol{B}\|_F^2} = \frac{b}{a+b+\varepsilon} \tag{2.6}$$

Where $\boldsymbol{A}$ and $\boldsymbol{B}$ are given in equations (2.3) and (2.4) respectively, $a = tr(\boldsymbol{A}^T\boldsymbol{A})$, $b = tr(\boldsymbol{B}^T\boldsymbol{B})$, and ε is a small positive number used to avoid division by zero.

Many researchers [1], [8], [10], [12], [32], and [40] are compared the Ω method with the previous vortex identification methods, and they are found that the Ω method is very successful in capturing the strong vortices as well as the weak ones. Besides capturing the vortices well and easy to perform, the Ω method has a clear physical meaning on the contrary to λ_2 and Q methods that provide an obscure interpretation by the iso-surface values them. Chosen $\Omega = 0.51$ or $\Omega = 0.52$ as the fixed threshold is investigated quantity that can always capture the vortices in different statuses and at different time steps while $\lambda_2$and Q need several thresholds to capture the vortex structure.

The designation of ε value in (2.6) is sensitive. In ref. [9], Dong defined ε in terms of the maximum of $b - a$, which is a fixed parameter at each time step in each case, as the following:

$$\varepsilon = 0.001\ (b-a)_{max} = 0.002\ Q_{max} \tag{2.7}$$

The second equality in (2.7) is obtained by apply (2.5). ε 's settlement, in many cases, becomes unnecessary by determining ε in the previous equation, but users still need to adjust ε for their computations.

2.3.2 Liutex based vortex identification methods

Liutex (previously known as Rortex) is a new concept that can be defined as a vector with direction, magnitude (scalar), and tensor forms which is proposed in 2018 by Professor Chaoqun Liu [15], [27], and [28]. The basic idea of the Liutex method is isolating the fluid rotation apart from other extraneous properties like shearing, which lets to determine the pure rotation of an incompressible fluid and allows for accurate interpretations of a vortex structure. Since vorticity can be decomposed into a rotational part and non-rotating part, vorticity can be expressed as:

$$\vec{\omega} = \nabla \times \vec{v} \; = \; \vec{R} + \vec{S} \tag{2.8}$$

Where $\vec{R}$ is Liutex and $\vec{S}$ is the antisymmetric shear. That means the Liutex vector is the rotational part of vorticity without shear contamination. The physical meaning of Liutex is introduced as Liutex is a vector, the direction of Liutex is the local rotation axis, and the magnitude of Liutex is twice the angular speed of local rigid rotation.

2.3.2.1 Liutex iso-surface

The iso-surface of Liutex magnitude can visualize the vortex structure since Liutex magnitude is a scalar value. However, the main difference between the Liutex iso-surface and the second generation methods iso-surface, such as λ_2 iso-surface, is that the rigid rotation is isolated of stretching and shearing contamination.

Definition 2.1. Liutex is defined as a rigid rotation part of fluid motion.

$$\vec{R} = R\,\vec{r} \tag{2.9}$$

and Liutex magnitude R explicitly expressed in [27] as:

$$R = (\vec{\omega} \cdot \vec{r}) - \sqrt{(\vec{\omega} \cdot \vec{r})^2 - 4{\lambda_{ci}}^2} \tag{2.10}$$

where, $\vec{r}$ is the real eigenvector of $\nabla\vec{v}$, $\vec{\omega} = \nabla \times \vec{v}$ is vorticity, and λ_{ci} is the imaginary part of the conjugate complex eigenvalues of $\nabla\vec{v}$. Since the normalized eigenvector is unique concerning the positive or negative sign, the condition $\vec{\omega} \cdot \vec{r} > 0$ maintains the definition's uniqueness and is consistent if the fluid motion is pure rotation. Based on the previous information, Liutex is reasonable because it is local, accurate, unique, systematical, and Galilean invariance.

Similar to the eigenvalues based methods, the Liutex iso-surface needs a threshold to be selected. That means the vortex structure depends on the user selection of the threshold: applying different threshold values will result in different vortex structures for the same data set, which is unacceptable; see Figure 2.4. As a result, the iso-surface is not sufficient to describe the vortex structure in the flow field.

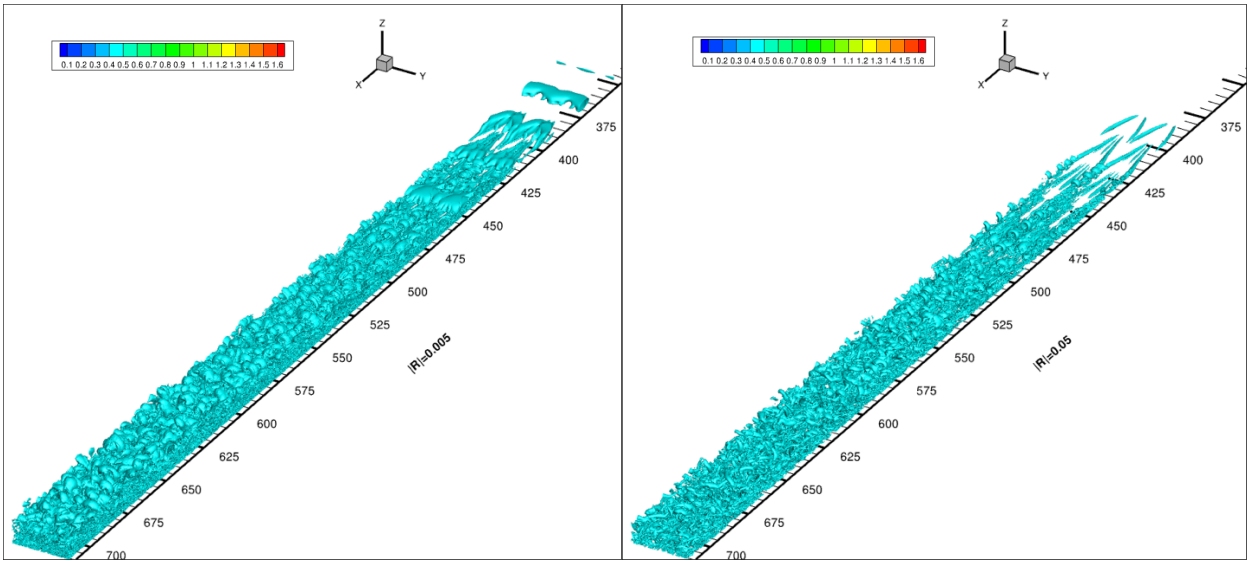

a)$|R| = 0.005$ b) $|R| = 0.05$

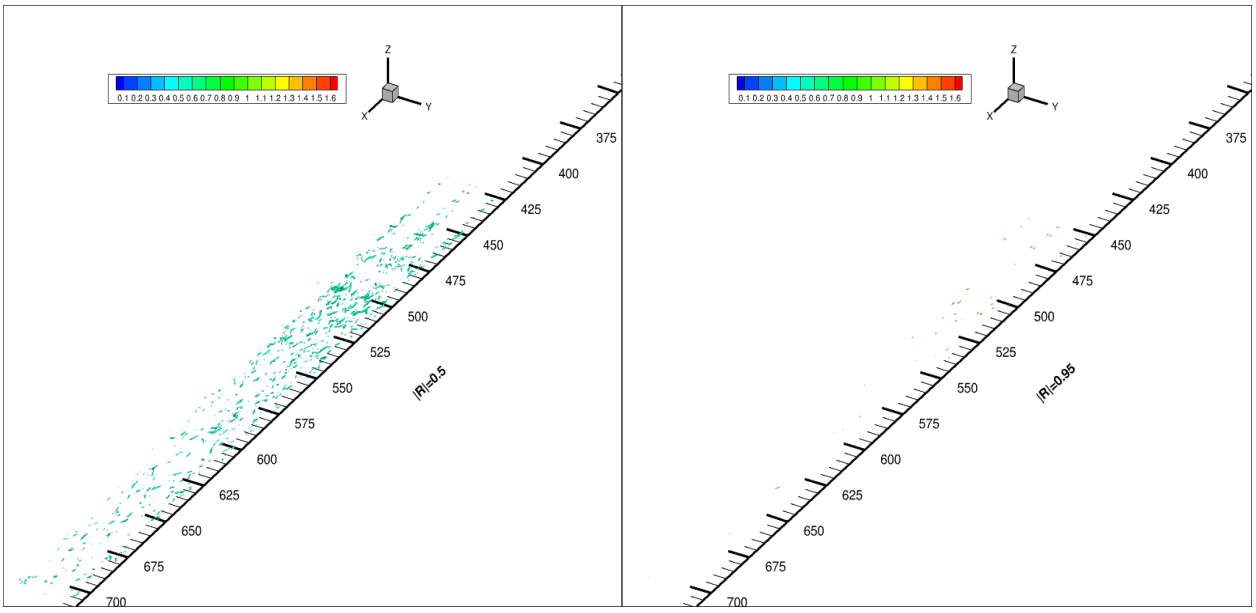

c) $|R| = 0.5$ d) $|R| = 0.95$

Figure 2.4: Liutex iso-surfaces with different thresholds for flow transition

2.3.2.2 Liutex core line

The vortex core line (or the vortex rotation axis) is the unique line that identifies the vortex's skeleton instead of using the iso-surface, which is highly affected by users' choice of the threshold. In [16], the Liutex core line's mathematical definition line is introduced as a line that satisfies that the Liutex magnitude gradient vector is aligned with the Liutex vector. The definition of the Liutex core line can be expressed as follows.

Definition 2.2. The Liutex core line (or the vortex rotation axis) can be defined as a Liutex line passing the points that satisfy the condition:

$$\nabla R \times \vec{r} = 0, \qquad R > 0 \tag{2.11}$$

where ∇R represents the Liutex magnitude gradient vector and $\vec{r}$ represents the direction of the Liutex vector.

This definition of the Liutex core line will be applied in Chapter 3 to find an automatic vortex structure identification method.

2.3.2.3 Liutex core tube

A bundle of Liutex lines is called a Liutex tube. If a Liutex Lines family is encircling the Liutex core line, they will take the same behavior and the vortex, which gives a prominent structure for the vortex that shows the strength or size.

Definition 2.3. The Liutex Core Tube can be defined as a collection of Liutex lines (finite or infinite amount) surrounding the Liutex core line.

The size of the Liutex core tube is decided by arbitrary percentage forms the radius of the tube. This percentage is chosen by the user, which means the Liutex core line is not unique because it depends on the users' choice of the tube size.

This definition of Liutex core tube will be applied in Chapter 4 to find an automatic vortex structures identification method.

2.3.3 Liutex- Ω vortex identification method

In 2019, Dong et al. [9] have combined the benefits of both Omega and Liutex methods in one method called the Liutex-Omega method. The Liutex- Ω method, Ω_R, is defined as the ratio of β squared over the sum of β squared and α squared as follows.

$$\Omega_R = \frac{\beta^2}{\alpha^2+\beta^2+\varepsilon} \tag{2.12}$$

Where

$$\alpha = \frac{1}{2}\sqrt{\left(\frac{\partial v}{\partial y} - \frac{\partial u}{\partial x}\right)^2 + \left(\frac{\partial v}{\partial x} + \frac{\partial u}{\partial y}\right)^2}, \tag{2.13}$$

$$\beta = \frac{1}{2}\left(\frac{\partial v}{\partial x} - \frac{\partial u}{\partial y}\right), \quad \text{and} \tag{2.14}$$

$$\varepsilon = b * (\beta^2 - \alpha^2)_{max} \tag{2.15}$$

where b is a small positive number around 0.001~0.002.

Dr. Liu's team found that the iso-surface of $\Omega_R = 0.52$ is the best choice to visualize the vortex structures clearly, see ref. [9] for more details. If Ω_R set as 0.52, Ω_R can simultaneously capture both weak and strong vortex structures compared with others vortex identification methods. Also, Ω_R can be applied for incompressible flow as well as compressible flow.

2.3.4 Modified Liutex-Omega method

In Liu et al. [27] (2019), the Liutex eigenvalue decomposition and Galilean invariance of Ω method revealed that

$$\nabla\vec{\boldsymbol{v}}_{\boldsymbol{\theta}\mathbf{min}} = \begin{bmatrix} \lambda_{cr} & -(\beta-\alpha) \\ \beta+\alpha & \lambda_{cr} \end{bmatrix} = \begin{bmatrix} \lambda_{cr} & \alpha \\ \alpha & \lambda_{cr} \end{bmatrix} + \begin{bmatrix} 0 & -\beta \\ \beta & 0 \end{bmatrix} = \boldsymbol{A} + \boldsymbol{B} \tag{2.16}$$

Where $\boldsymbol{A}$ and $\boldsymbol{B}$ are given in (2.3) and (2.4) respectively. Also, β and α are given in (2.13) and (2.14), respectively, in the last section. By applying (2.16) in (2.6), the following equation given.

$$\Omega_{2\mathrm{D}} = \frac{b}{a+b+\epsilon} = \frac{\beta^2}{\beta^2+\alpha^2+\lambda_{cr}^2+\epsilon} \tag{2.17}$$

Similarly,

$$\nabla\vec{\boldsymbol{v}}_{\boldsymbol{\theta}\mathbf{min}} = \begin{bmatrix} \lambda_{cr} & -(\beta-\alpha) & 0 \\ \beta+\alpha & \lambda_{cr} & 0 \\ \xi & \eta & \lambda_r \end{bmatrix} = \begin{bmatrix} \lambda_{cr} & \alpha & \frac{1}{2}\xi \\ \alpha & \lambda_{cr} & \frac{1}{2}\eta \\ \frac{1}{2}\xi & \frac{1}{2}\eta & \lambda_r \end{bmatrix} + \begin{bmatrix} 0 & -\beta & -\frac{1}{2}\xi \\ \beta & 0 & -\frac{1}{2}\eta \\ \frac{1}{2}\xi & \frac{1}{2}\eta & 0 \end{bmatrix} = \boldsymbol{A} + \boldsymbol{B} \qquad (2.18)$$

Then,

$$\Omega_{3D} = \frac{\beta^2+\frac{1}{4}(\xi^2+\eta^2)}{\beta^2+\frac{1}{2}(\xi^2+\eta^2)+\alpha^2+\lambda_{cr}^2+\frac{1}{2}\lambda_{cr}^2+\epsilon} \qquad (2.19)$$

From (2.17) and (2.19), the Ω method is different than what is defined in section **2.3.3**. Based on this idea, Liu, Jianming and Liu, Chaoqun [34] have proposed the modified normalized Liutex/vortex identification method.

$$\widetilde{\Omega}_R = \frac{\beta^2}{\beta^2+\alpha^2+\lambda_{cr}^2+\frac{1}{2}\lambda_r^2+\epsilon} \qquad (2.20)$$

According to [34], setting $\widetilde{\Omega}_R = 0.52$ as the fixed threshold is always appropriate and can capture both solid and weak vortices. Moreover, $\widetilde{\Omega}_R$ can keep the ring structures of the threshold is increased with the high relative strength of vortex structures in different places. Thus, the modified Liutex-Omega method, $\widetilde{\Omega}_R$, is the best iso-surface-based vortex identification method until now; see Figure 2.5 and Figure 2.6.

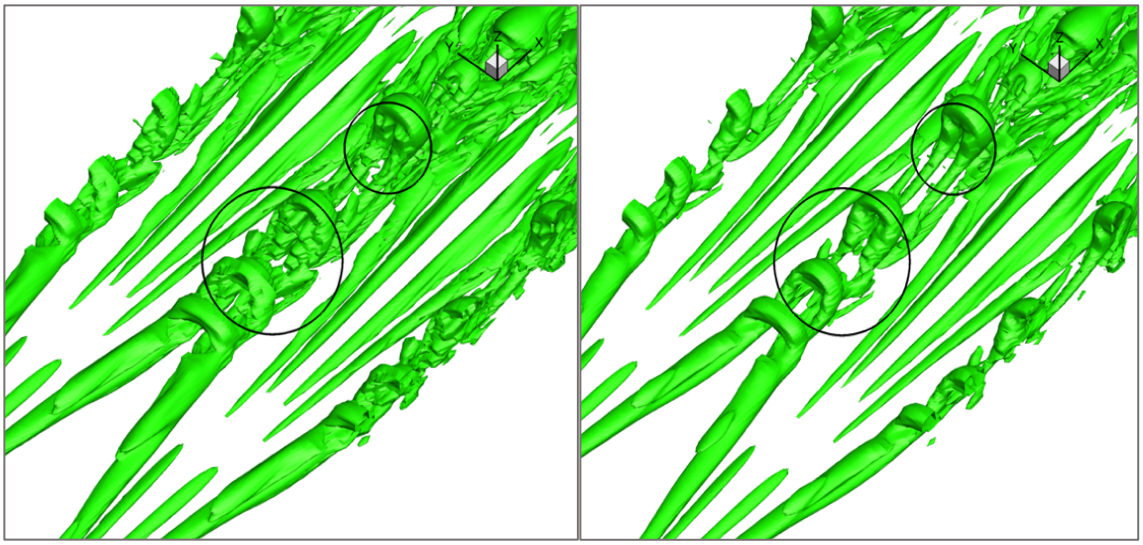

a)Ω_R method b) $\widetilde{\Omega}_R$ method

Figure 2.5: The iso-surfaces of hairpin vortex structures for both Ω_R and $\widetilde{\Omega}_R$ methods

Since the modified Liutex-Omega method is the best vortex identification method that can capture both strong and weak vortices at the same time very well, the modified Liutex-Omega with $\widetilde{\Omega}_R = 0.52$ will be used to extract the local maximum points in this dissertation; see chapter 3.

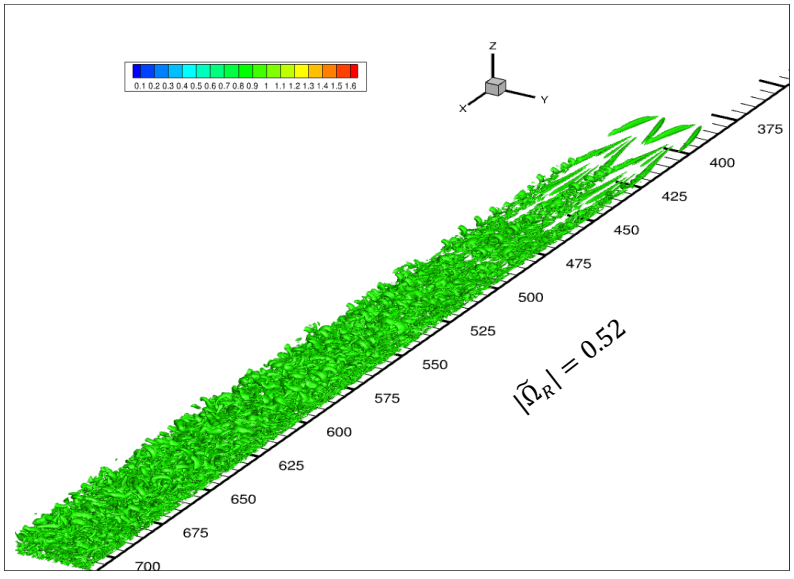

Figure 2.6: The iso-surfaces of modified Liutex-Omega with $\widetilde{\Omega}_R = 0.52$

2.3.5 The Liutex method advantages

Liutex method provides enough information that solves many problems related to vortex identification. Unlike the first and second generations methods, the Liutex method is the only method that can answer six essential issues of vortex definition and identification which are:1)What is the absolute strength of a vortex? 2)What is the relative strength of a vortex? 3)What is the rotation axis? 4)Where is the vortex core center? 5)What is the size of the vortex core? 6)Where is the vortex core boundary? The answers to the previous questions can be stated as follows[41].

2.3.5.1 The absolute strength of the vortex

Based on Gao et al.[13], Liutex magnitude is the absolute strength. Since the definition of Liutex magnitude is stated as twice the angular speed of the rigid rotation part of the fluid motion, Liutex magnitude is the best measurement of the rigid rotation part because it is not contaminated by shearing like others methods.

2.3.5.2 The relative strength of the vortex

The relative strength means here the Liutex density or the fluid motion solidity. It can be addressed by Liutex-Omega\ modified Liutex-Omega methods since they can capture both the strong and weak vortices simultaneously, unlike Liutex, which is absolute strength; so it may fail to capture the weak vortices. For this reason, Liutex-Omega is the best iso-surfaces visualization method of vortex based on many user reviews.

2.3.5.3 The vortex core center

The Liutex vector direction is in the local rotational axis. From the definition of Liutex, it is known that the local rotational axis is in the local real eigenvector of velocity gradient tensor direction, where the other two corresponding eigenvalues are complex conjugate. This information about the local axis direction allows us to create smooth Liutex lines, which have an essential role in extracting the vortex cores.

2.3.5.4 The rotation axis

From definition 2.2, both the Liutex vector and the gradient of Liutex magnitude have the same direction. That means vortex cores can be determined where Liutex magnitude is locally maximum in the plane normal to r. In chapter 3, this condition will be used to find an exact algorithm that produces the Liutex core line.

2.3.5.5 The size of the vortex core

From section 2.3.2.3, the vortex core size directly depends on the Liutex core line and the vortex core center, which region is the central region where fluid rotation happens. In chapter 4, an exact algorithm to create a Liutex core tube, which shows the vortex's size, will be presented in detail.

2.3.5.6 The vortex core boundary

The separation line (or separation surface) between the rotation and non-rotation area in the vortex is called the vortex boundary, so this area combines rotation and shearing. The second-generation vortex identification methods use a non-zero threshold to define the boundary

of vortices which is arbitrary and subjective selection depends on the users. Therefore, applying the iso-surface of $\Omega_R = 0.52$(or $\widetilde{\Omega}_R = 0.52$) can guarantee a clear appearance to various flows without changing of thresholds each time.

In this dissertation, the researcher will answer two profound questions: (1) Where is the rotation axis? Furthermore, (2) What is the size of the vortex core? In chapter 3, the researcher will propose an algorithm to find the Liutex core center points, i.e., the local maxima points, and determine the Liutex core line. In chapter 4, the researcher will introduce an algorithm to locate a Liutex core tube that shows the vortex structure and strength.

2.4 Summary:

This chapter discusses the three different generations of vortex identification methods. The first generation that based on vorticity that established by Helmholtz and his three vortex theorems. However, several sensible arguments refute allegations of Helmholtz's vortex definition and his theorems have been explained. The second generation of vortex identification methods that are eigenvalue-based includes Q-criterion, Δ-criterion, λ_{ci}-criterion, and λ_2-criterion was discussed in the next section. Since Q-criterion and λ_2-criterion are the most commonly used in the second generation, the researcher covered them in minor detail. The limitations of the second-generation methods are underlined clearly. Finally, the third generation of vortex identification methods that include Omega, Liutex, Liutex-Omega, and modified Liutex-Omega methods are presented. The power of the Liutex method was highlighted by providing the answer for the six essential issues of vortex identification methods that are: 1)The absolute strength of a vortex, 2) The relative strength of a vortex, 3) The vortex core center, 4) The rotation axis, 5) The size of the vortex core, and 6) The vortex core boundary.

CHAPTER 3

AN AUTOMATIC METHOD FOR FINDING THE LIUTEX CORE LINE

This chapter will propose an automatic method to find the Liutex core line to visualize the vortices structure. Therefore, it is organized as follows. First, the Liutex lines will be defined, and the difference between Liutex lines and the vorticity lines will be clarified. The Liutex core line will then be introduced automatically by determining the local maxima points using the modified Liutex-Omega method; $\widetilde{\Omega}_R$, then draw the Liutex line through these points. The critical step to do so is finding the best local maxima points, which need to satisfy several conditions. Some conditions will apply to nominate the number of the seed points in the following sections. After that, the automatic Liutex core line algorithm will be outlined dependent on clear and reasonable mathematical explanations. Finally, the summary of finding the core line's automated method is given in the last section.

3.1 Liutex lines vs vorticity lines

Liutex being a vector allows to defined Liutex lines everywhere. Liutex line is a line that is tangent to the local Liutex vector. In Chapter 2, It has been shown that vorticity cannot represent vortex. It has been found that: near the wall of a laminar boundary layer, vorticity is very large where there is no fluid rotation or vortex. Figure 3.1 shows vorticity lines and Liutex lines have been drawn through Λ-vortex [41] with and without iso-surfaces. It is clear to see that the vorticity lines penetrate vortex structures, but they are not aligned along while the Liutex lines are covered by the Λ-vortex iso-surface almost precisely.

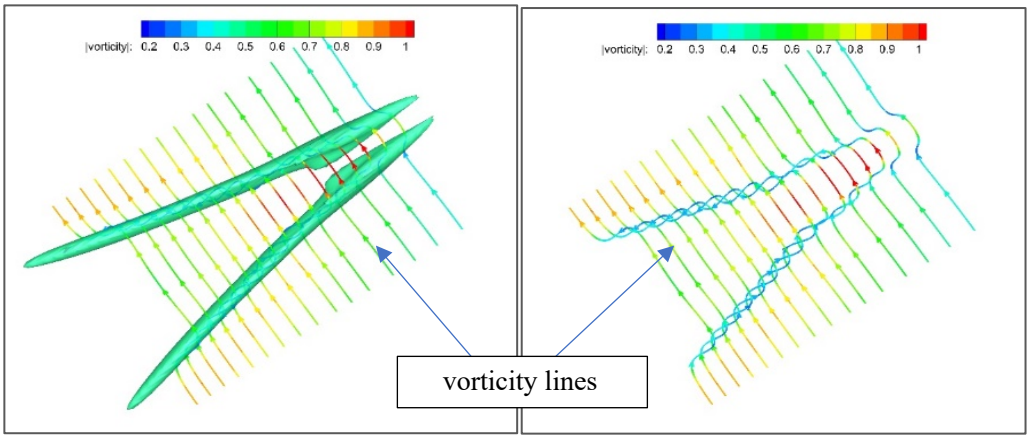

(a) with iso-surface without iso-surface

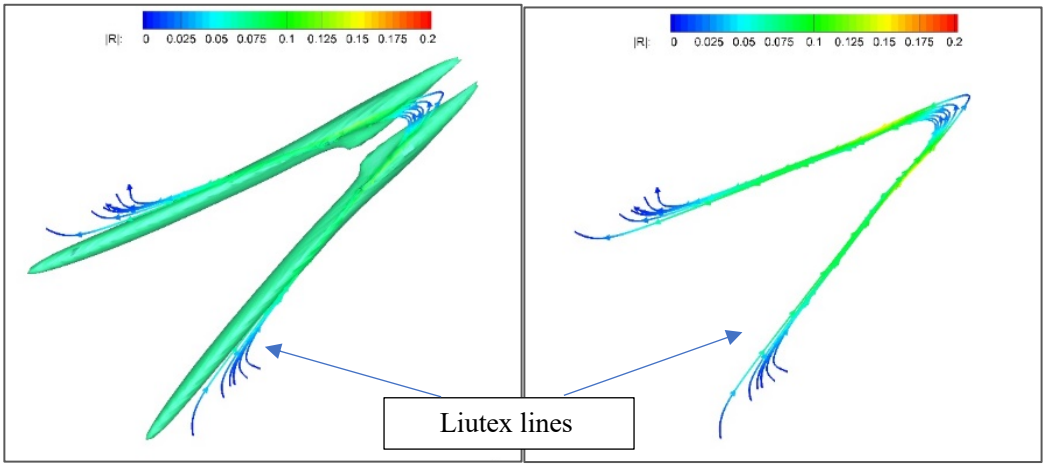

(b) with iso-surface without iso-surface

Figure 3.1: Vorticity lines and Liutex lines through the Λ-vortex

Figure 3.2 shows a similar case to the hairpin vortex. Also, It can be noticed that the vorticity concentration does not follow the vortex location most of the time. The next section will propose an exact algorithm to construct the unique Liutex core line, dependent on clear and reasonable mathematical explanations [30].

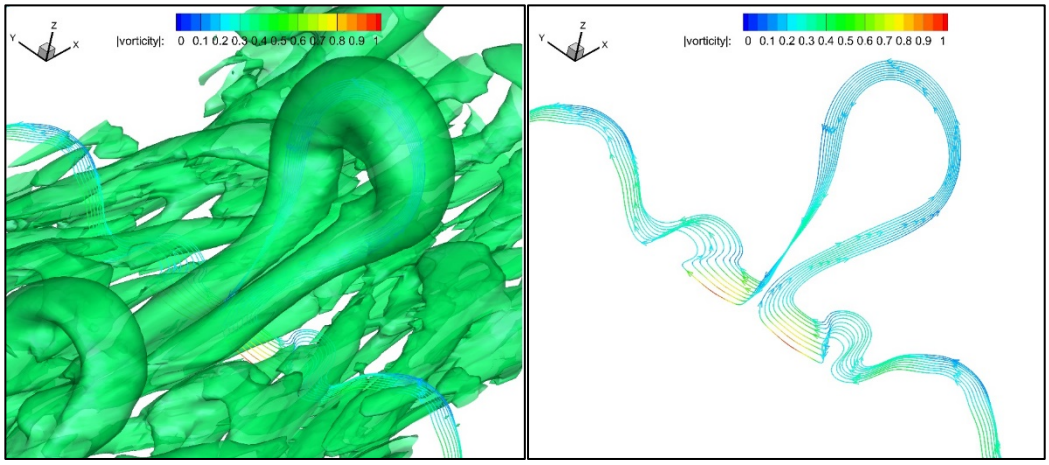

(a) with iso-surface without iso-surface

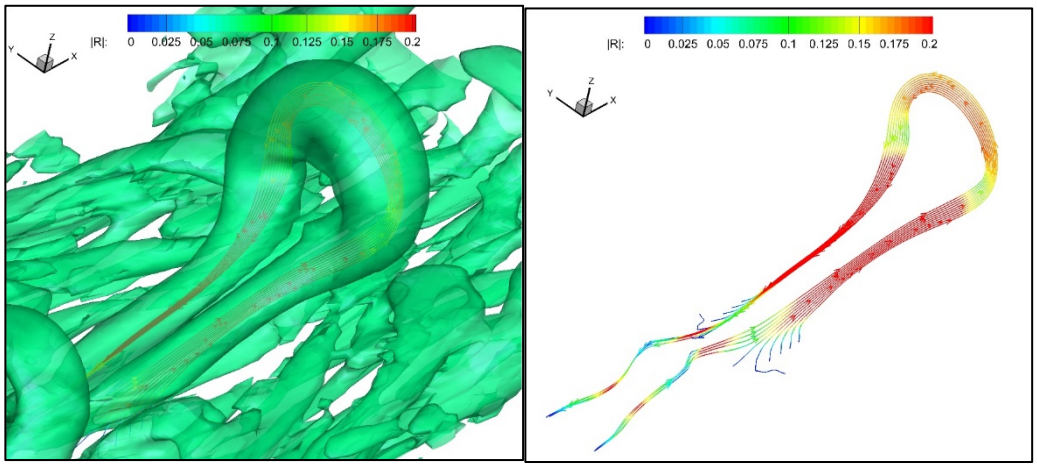

(b) with iso-surface without iso-surface

Figure 3.2: Vorticity lines and Liutex lines through the hairpin vortex

3.2 An automatic method for finding Liutex core line

This section answers one of the essential issues, as stated in chapter 2, to identify the vortex, the rotation axis(Liutex core line) location. First, find the best local maximum points using the modified Liutex-Omega, which is the most tricky and sensitive step. Then, draw the Liutex line through these points.

One of the advantages of Liutex is being a vector instead of just a scalar. That allows finding the center axis of the vortex rotation, which can help set the vortex structure. All Liutex gradient lines converge to one concentration line by observation, which is judged to be the vortex rotation axis line as the local Liutex maxima on the plane perpendicular to the vortex rotation axis line. So, starting the automated method by finding the local maximum points will be the first step. To do so, we need to find all the seed points, even for weak vortices. Then, filter the unnecessary seed points, which could make noises everywhere. The following subsections show all steps in details:

3.2.1 Setting the modified Liutex-Omega method; $\widetilde{\Omega}_R$

According to the discussion in chapter 2, the modified Liutex-Omega method has several advantages over other methods. Without shear contamination, the modified Liutex-Omega method can capture both weak and robust vortices simultaneously. The modified Liutex-Omega method is insensitive to the threshold change; setting $\widetilde{\Omega}_R = 0.52$ is the best choice; see figure 2.6. The modified Liutex-Omega with $\widetilde{\Omega}_R = 0.52$ is applied as the first rule in this algorithm. This condition is used to exclude the non-vortex points.

3.2.2 Finding the core center-points (the local maximum points)

Definition 3.1. The vortex core center-point can be defined as the concentration of gradient of Liutex lines, i.e., the local maxima [16].

The critical point of any function f is the value p that belongs to the function's domain and satisfies that f is not differentiable at p or its differentiable at p is zero.

Definition 3.2. Consider p be an interior point in the domain of the function f. p is a critical point of f if $f'(p) = 0$ or $f'(p)$ is undefined [19].

There are three different types of the critical point of any function: local maximum point, local minimum point, and saddle point. The local maximum point is a point p in the function's domain such that all other points in a neighborhood near to p produce smaller values when all these points are implemented through the function. See figure 3.3 [3], which shows the physical meaning of the three different types.

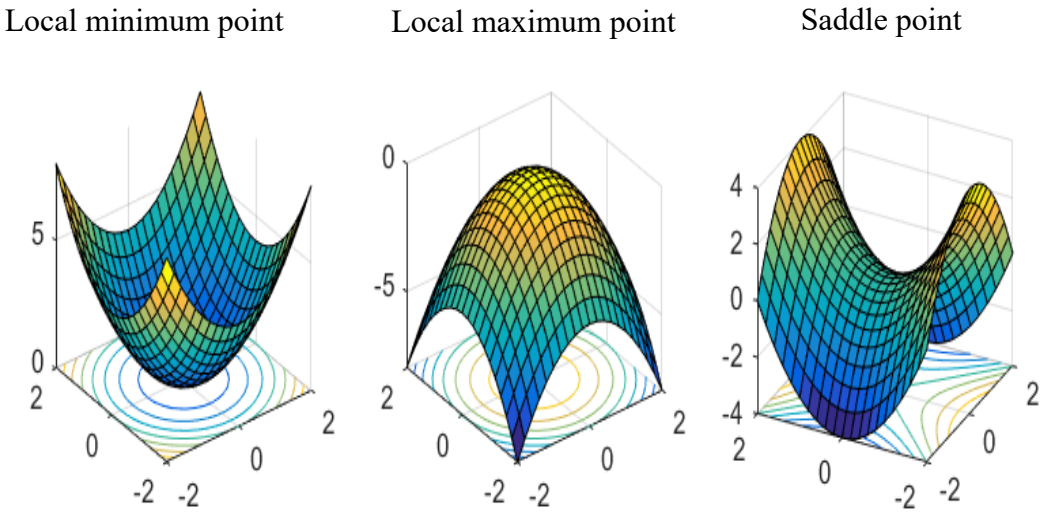

Figure 3.3: Three different types of the critical point

In practice, to find a local maximum point at some neighborhood of a function, we need to select all extrema points in this region first then test them to find the highest value after the function has effectuated. The second derivative test will be used in the current case, ref.[22].

3.2.2.1 The second derivative test

From the definition of the modified Liutex-Omega, it has been known that $\widetilde{\Omega}_R$ is differentiable; the second partial derivative of $\widetilde{\Omega}_R$ exists and continuous on its domain; see chapter 2. Let $p = (x, y, z)$ be a point belong to $\widetilde{\Omega}_R$ domain. If :

- $\nabla\widetilde{\Omega}_R = 0$, i.e.: since $\nabla\widetilde{\Omega}_R = \begin{bmatrix} \frac{\partial\widetilde{\Omega}_R}{\partial x} \\ \frac{\partial\widetilde{\Omega}_R}{\partial y} \\ \frac{\partial\widetilde{\Omega}_R}{\partial z} \end{bmatrix} = \begin{bmatrix} 0 \\ 0 \\ 0 \end{bmatrix}$. So, it is needed to set:

  $$\frac{\partial\widetilde{\Omega}_R}{\partial x} = 0,\ \frac{\partial\widetilde{\Omega}_R}{\partial y} = 0,\ \text{and}\ \frac{\partial\widetilde{\Omega}_R}{\partial z} = 0 \quad \text{, and} \tag{3.1}$$

- Hessian matrix, H, of the second partial derivatives with respect to $\widetilde{\Omega}_R$ is negative definite at the same point , i.e.: $p^T H\, p < 0,\ \forall\, p \neq 0.$ (3.2)

are satisfied. Then, $p = (x, y, z)$ is a local maximum point of $\widetilde{\Omega}_R$.

For simplified the previous condition, it is needed to answer the question: How will it check whether H is negative definite at the critical point p or not? There are many ways to do so, such as if all the Hessian matrix eigenvalues are negative at p, then p is a local maximum point. Even though the eigenvalue test is useful theoretically, it is not easy to apply in practice because computing eigenvalues is expensive somehow while it is needed to reduce the cost of the competition as possible for more accurate and faster results. So, the following steps will show a more painless technique to check that.

Assume that the Hessian matrix, $H = \begin{bmatrix} \frac{\partial^2 \widetilde{\Omega}_R}{\partial x^2} & \frac{\partial^2 \widetilde{\Omega}_R}{\partial x \partial y} & \frac{\partial^2 \widetilde{\Omega}_R}{\partial x \partial z} \\ \frac{\partial^2 \widetilde{\Omega}_R}{\partial x \partial y} & \frac{\partial^2 \widetilde{\Omega}_R}{\partial y^2} & \frac{\partial^2 \widetilde{\Omega}_R}{\partial y \partial z} \\ \frac{\partial^2 \widetilde{\Omega}_R}{\partial x \partial z} & \frac{\partial^2 \widetilde{\Omega}_R}{\partial y \partial z} & \frac{\partial^2 \widetilde{\Omega}_R}{\partial z^2} \end{bmatrix}$ is symmetric, i.e.: $H^T = H$.

Notice that the Hessian matrix is not symmetric in general. Consider the principal minor method of H as follows. Let H be an $n \times n$ symmetric matrix and let H_k be the submatrix of H obtained by taking the upper left-hand corner $k \times k$ submatrix of H. Furthermore, let $\Delta k = \det(H_k)$ the k^{th} principal minor of H. Then, H is negative definite if and only if $(-1)^k \Delta k > 0$ for $k = 1,2, \dots, n$. That means; in the current case, if the following :

- $\det\left(\frac{\partial^2 \widetilde{\Omega}_R}{\partial x^2} \right) < 0$, i.e.: $\frac{\partial^2 \widetilde{\Omega}_R}{\partial x^2} < 0$, (3.3)
- $\det \begin{bmatrix} \frac{\partial^2 \widetilde{\Omega}_R}{\partial x^2} & \frac{\partial^2 \widetilde{\Omega}_R}{\partial x \partial y} \\ \frac{\partial^2 \widetilde{\Omega}_R}{\partial x \partial y} & \frac{\partial^2 \widetilde{\Omega}_R}{\partial y^2} \end{bmatrix} > 0$, and (3.4)
- $\det \begin{bmatrix} \frac{\partial^2 \widetilde{\Omega}_R}{\partial x^2} & \frac{\partial^2 \widetilde{\Omega}_R}{\partial x \partial y} & \frac{\partial^2 \widetilde{\Omega}_R}{\partial x \partial z} \\ \frac{\partial^2 \widetilde{\Omega}_R}{\partial x \partial y} & \frac{\partial^2 \widetilde{\Omega}_R}{\partial y^2} & \frac{\partial^2 \widetilde{\Omega}_R}{\partial y \partial z} \\ \frac{\partial^2 \widetilde{\Omega}_R}{\partial x \partial z} & \frac{\partial^2 \widetilde{\Omega}_R}{\partial y \partial z} & \frac{\partial^2 \widetilde{\Omega}_R}{\partial z^2} \end{bmatrix} < 0$ (3.5)

are satisfied, then $p = (x, y, z)$ is a local maximum point.

The second derivative test calculates all the local maximum points even for the weak vortices, which will result from a massive bunch of local maximum points. The result never gives the unique Liutex core line that needed to find. So there is a needs to move away from the weak local max points and keep only the core line points.

3.2.3 Using the definition of Liutex core line (rotation axis)

Recalling the definition of Liutex core line, definition 2.2 in chapter 2, the Liutex core Line (rotation axis) is a Liutex line where all the points belonging to it satisfy the equation (2.11). The vortex's rotation axis definition based on the Liutex vector allows the best way to represent the vortices by Liutex core lines that are colored according to the vortex strength. The equation (2.11) means that the gradient of Liutex has the same direction as the local Liutex vector, which is $\vec{r}$. Moreover, ∇R is perpendicular to any line element $\overrightarrow{dl}$. The next theorems explain the idea behind definition (2.11) [43].

Definition 3.3: A Liutex (vortex) rotation axis line is defined as the local maxima of Liutex, which is a line without iso-surface.

Theorem 3.1: If $\nabla R \neq 0$, then any small element of a line; say $\overrightarrow{dl}$, on the Liutex iso-surface must be orthogonal to the gradient of Liutex.

Proof: On the Liutex iso-surface, $dR = \nabla R \cdot \overrightarrow{dl} = 0$, that means $\overrightarrow{dl}$ and ∇R are orthogonal. ■

Theorem 3.2: If $\nabla R \times \overrightarrow{dl} = 0$ at a point p, then p must belong to the Liutex rotation axis.

Proof: Consider the point s that is not located in the Liutex rotation core axis. Then s has to be on some Liutex iso-surface. If $\overrightarrow{dl}$ is also on a Liutex iso-surface, then $\mathrm{dR} = \nabla R \cdot \overrightarrow{dl} = 0$ must hold at s and then $\nabla R \times \overrightarrow{dl} \neq 0$. On the other hands, if $\nabla R \times \overrightarrow{dl} = 0$, $\overrightarrow{dl}$ not on any Liutex iso- surface, which is the Liutex rotation axis because according to Definition 3.3, the Liutex rotation axis is a local maxima and has no Liutex iso-surface. ■

To apply (2.11) in practice, it is need to set the result of the cross product of $\nabla\widetilde{\Omega}_R$ and $\vec{r}$ to be zero. That means, if $\vec{r} = \begin{bmatrix} r_1 \\ r_2 \\ r_3 \end{bmatrix}$ is the real eigenvector of $\nabla\vec{v}$ and $\nabla\widetilde{\Omega}_R = \begin{bmatrix} \frac{\partial\widetilde{\Omega}_R}{\partial x} \\ \frac{\partial\widetilde{\Omega}_R}{\partial y} \\ \frac{\partial\widetilde{\Omega}_R}{\partial z} \end{bmatrix}$ is the gradient of the modified Liutex-Omega, then

$$\nabla\widetilde{\Omega}_R \times \vec{r} = \begin{bmatrix} \frac{\partial\widetilde{\Omega}_R}{\partial x} \\ \frac{\partial\widetilde{\Omega}_R}{\partial y} \\ \frac{\partial\widetilde{\Omega}_R}{\partial z} \end{bmatrix} \times \begin{bmatrix} r_1 \\ r_2 \\ r_3 \end{bmatrix} = \det \begin{bmatrix} \hat{\imath} & \hat{\jmath} & \hat{k} \\ \frac{\partial\widetilde{\Omega}_R}{\partial x} & \frac{\partial\widetilde{\Omega}_R}{\partial y} & \frac{\partial\widetilde{\Omega}_R}{\partial z} \\ r_1 & r_2 & r_3 \end{bmatrix}$$

$$= \det \begin{bmatrix} \frac{\partial\widetilde{\Omega}_R}{\partial y} & \frac{\partial\widetilde{\Omega}_R}{\partial z} \\ r_2 & r_3 \end{bmatrix} \hat{\imath} - \det \begin{bmatrix} \frac{\partial\widetilde{\Omega}_R}{\partial x} & \frac{\partial\widetilde{\Omega}_R}{\partial z} \\ r_1 & r_3 \end{bmatrix} \hat{\jmath} + \det \begin{bmatrix} \frac{\partial\widetilde{\Omega}_R}{\partial x} & \frac{\partial\widetilde{\Omega}_R}{\partial y} \\ r_1 & r_2 \end{bmatrix} \hat{k}$$

$$= \left(\frac{\partial\widetilde{\Omega}_R}{\partial y} r_3 - \frac{\partial\widetilde{\Omega}_R}{\partial z} r_2\right)\hat{\imath} - \left(\frac{\partial\widetilde{\Omega}_R}{\partial x} r_3 - \frac{\partial\widetilde{\Omega}_R}{\partial z} r_1\right)\hat{\jmath} + \left(\frac{\partial\widetilde{\Omega}_R}{\partial x} r_2 - \frac{\partial\widetilde{\Omega}_R}{\partial y} r_1\right)\hat{k} \quad (3.6)$$

The equation (2.11) can be rewritten using the expression (3.6) as the follows.

$$\nabla\widetilde{\Omega}_R \times \vec{r} = \begin{bmatrix} \frac{\partial\widetilde{\Omega}_R}{\partial y} r_3 - \frac{\partial\widetilde{\Omega}_R}{\partial z} r_2 \\ \frac{\partial\widetilde{\Omega}_R}{\partial z} r_1 - \frac{\partial\widetilde{\Omega}_R}{\partial x} r_3 \\ \frac{\partial\widetilde{\Omega}_R}{\partial x} r_2 - \frac{\partial\widetilde{\Omega}_R}{\partial y} r_1 \end{bmatrix} = \begin{bmatrix} 0 \\ 0 \\ 0 \end{bmatrix}$$

i.e: $$\begin{cases} \frac{\partial\widetilde{\Omega}_R}{\partial y} r_3 - \frac{\partial\widetilde{\Omega}_R}{\partial z} r_2 = 0 \\ \frac{\partial\widetilde{\Omega}_R}{\partial z} r_1 - \frac{\partial\widetilde{\Omega}_R}{\partial x} r_3 = 0 \\ \frac{\partial\widetilde{\Omega}_R}{\partial x} r_2 - \frac{\partial\widetilde{\Omega}_R}{\partial y} r_1 = 0 \end{cases}$$

So that :

$$\frac{\partial\widetilde{\Omega}_R}{\partial y} r_3 = \frac{\partial\widetilde{\Omega}_R}{\partial z} r_2 \quad (3.7)$$

$$\frac{\partial\widetilde{\Omega}_R}{\partial z} r_1 = \frac{\partial\widetilde{\Omega}_R}{\partial x} r_3 \quad (3.8)$$

$$\frac{\partial\widetilde{\Omega}_R}{\partial x} r_2 = \frac{\partial\widetilde{\Omega}_R}{\partial y} r_1 \quad (3.9)$$

That means, all the points that belong to the Liutex core line are satisfy the equations (3.7), (3.8), and (3.9). Even though the equation (2.11) has been proved mathematically as stated above, ref. [43], in practice, it is possible to find some points that satisfy (2.11) and do not belong to the Liutex core line for many reasons, which will be discussed later in this chapter. So, to filter the fake maximum points, the expression of the convective derivative of modified Liutex-Omega will be used in the following condition.

3.2.4 Using the convective derivative

The material derivative is a mathematical relationship that relates the time rate of change of a physical quantity, which is Liutex in our case, as observed from the Lagrangian viewpoint to the time rate of changing the same physical quantity as observed from the Eulerian viewpoint. So based on this meaning, the full derivative expression from the Eulerian point of view is

$$\left(\frac{D\widetilde{\Omega}_R}{Dt}\right)_p = \frac{\partial\widetilde{\Omega}_R}{\partial t} + u\frac{\partial\widetilde{\Omega}_R}{\partial x} + v\frac{\partial\widetilde{\Omega}_R}{\partial y} + w\frac{\partial\widetilde{\Omega}_R}{\partial z} \tag{3.10}$$

where $\frac{D\widetilde{\Omega}_R}{Dt}$ is the total rate of change in $\widetilde{\Omega}_R$ observed by a fluid element p, $\frac{\partial\widetilde{\Omega}_R}{\partial t}$ it is called the unsteady term, which is the rate of change in $\widetilde{\Omega}_R$ with respect to the time, and $\vec{v}\cdot\nabla\widetilde{\Omega}_R$ is called the convective term, which is the rate of change in R with respect to the space.

In 2020, Wang et al. [42] has proposed an expression of the convective derivative of (3.10) given as follows.

$$\frac{D\widetilde{\Omega}_R}{Dt} = \frac{\partial\widetilde{\Omega}_R}{\partial t} + \widetilde{\Omega}_R\nabla\cdot\vec{v} + \vec{v}\cdot\nabla\widetilde{\Omega}_R - \nabla\times\left(\vec{v}\times\widetilde{\Omega}_R\right) \tag{3.11}$$

where:

- $\widetilde{\Omega}_R\nabla\cdot\vec{v}$ is Liutex stretching term (LST), which represents the normal strain of vortex axis.

- $\vec{v} \cdot \nabla \widetilde{\Omega}_R$ is Liutex dilatation term (LDT), which represents the effects of Liutex divergence in the convection process.
- $-\nabla \times \left(\vec{v} \times \widetilde{\Omega}_R\right)$ is Liutex curl term (LCT), which represents the effects of shearing motion and local acceleration.

Since the Liutex core line is in isolation of the effects of Liutex divergence in the convection process and shearing motion and local acceleration, LDT and LCT are needs to vanished, which means the only term that is remained in (3.11) is the LST. In practice, there is a needs to simplify the following. Since there is nothing special with p, (3.11) can be written as

$$\frac{D\widetilde{\Omega}_R}{Dt} = \frac{\partial \widetilde{\Omega}_R}{\partial t} + \widetilde{\Omega}_R \nabla \cdot \vec{v} \tag{3.12}$$

By apply (3.10),

$$\frac{\partial \widetilde{\Omega}_R}{\partial t} + u\frac{\partial \widetilde{\Omega}_R}{\partial x} + v\frac{\partial \widetilde{\Omega}_R}{\partial y} + w\frac{\partial \widetilde{\Omega}_R}{\partial z} = \frac{\partial \widetilde{\Omega}_R}{\partial t} + \widetilde{\Omega}_R \nabla \cdot \vec{v}$$

$$u\frac{\partial \widetilde{\Omega}_R}{\partial x} + v\frac{\partial \widetilde{\Omega}_R}{\partial y} + w\frac{\partial \widetilde{\Omega}_R}{\partial z} = \widetilde{\Omega}_R \nabla \cdot \vec{v}$$

i.e: $\vec{v} \cdot \nabla \widetilde{\Omega}_R = \widetilde{\Omega}_R \nabla \cdot \vec{v}$ (3.13)

So for filtering the local max points, it could be apply (3.13) or set LDT and LCT to be zero.

3.3 Algorithm of the automatic method for finding the unique Liutex core line

In this section, the algorithm of extraction the unique Liutex core line automatically will be summarized as follows.

Algorithm 3.1: Finding the Liutex core line

Rule 1: Set the modified Liutex-Omega threshold to be 0.52; $\widetilde{\Omega}_R = 0.52$ to exclude the non-vortex points when $\widetilde{\Omega}_R < 0.52$.

Rule 2: Find all the core center points (the local maxima points) for both strong and weak vortices using the second derivative test by apply (3.1), (3.3), (3.4), and (3.5).

Rule 3: Filter these local maximum points using the definition of Liutex core line by apply (3.7), (3.8), and (3.9).

Rule 4: Force more conditions on these local maxima points to exclude fake points as much as possible, using the convective derivative decomposition by apply (3.13).

Rule 5: Draw the Liutex lines through the points that are obtained from the previous steps to extract the Liutex core line.

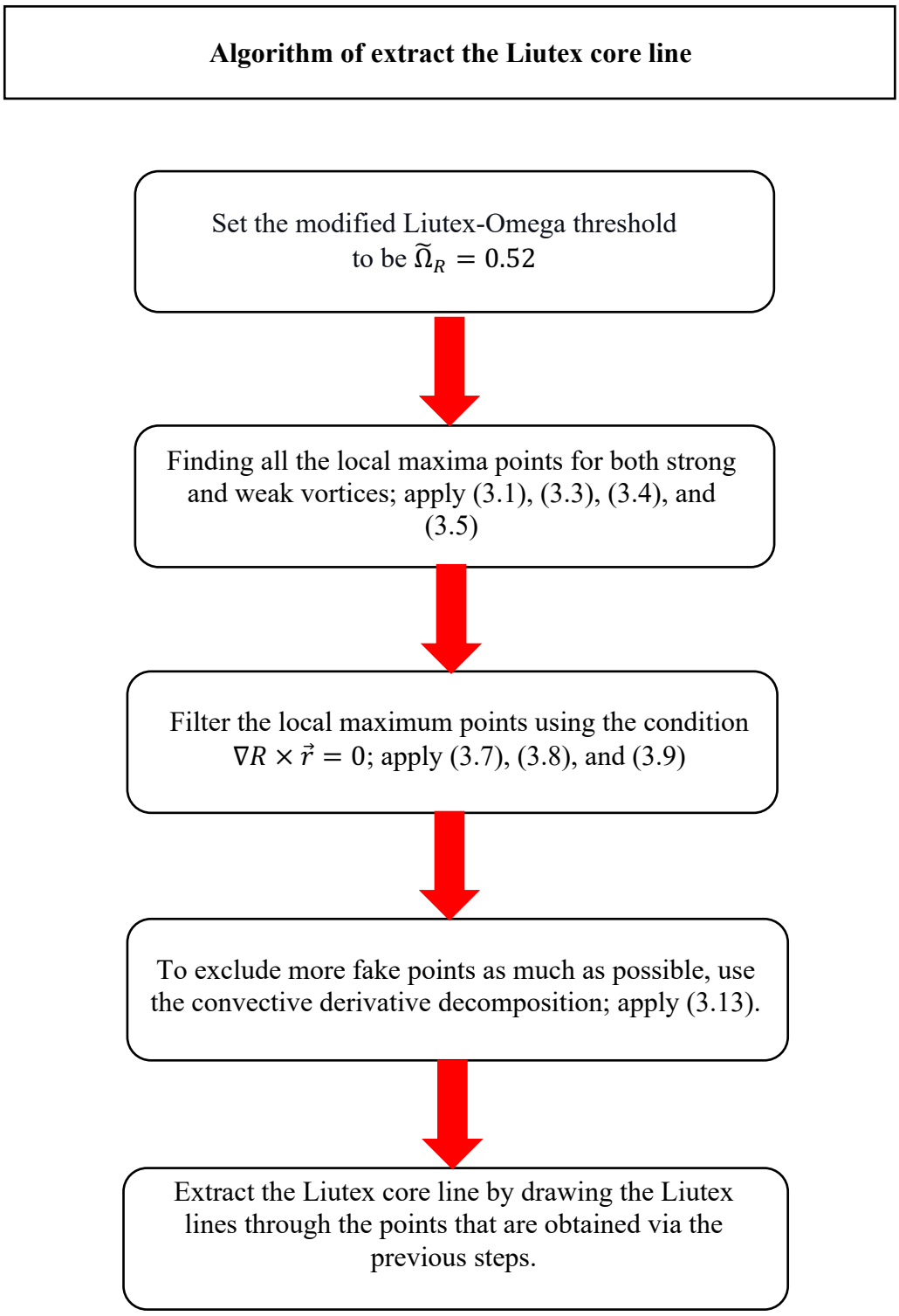

Figure 3.4: An algorithm of finding the Liutex core line

3.4 The numerical result: testing case

In this section, the proposed automatic method is applied to find the Liutex core line for the data obtained from a Direct Numerical Simulation (DNSUTA) of flow transition in boundary layers validated by researchers from UTA and NASA Langley, see chapter 1.

Figure 3.5 and Figure 3.6 show the local maximum points before and after drawing the Liutex line. It is clear to see that the Liutex core line passes through the local maximum points, which have been calculated by algorithm 3.1.

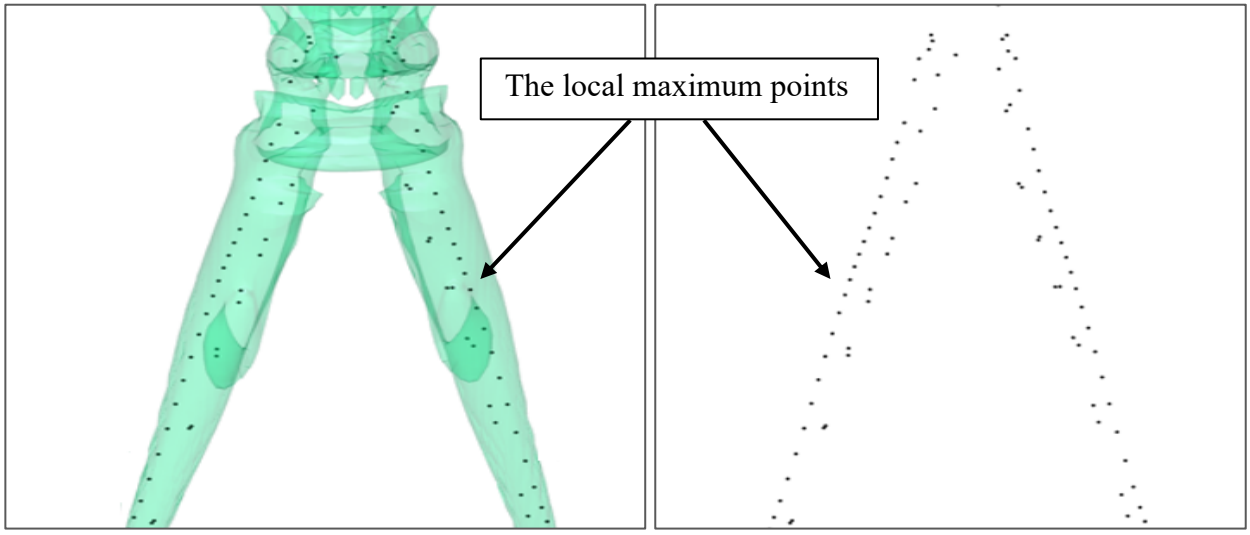

a) with iso-surface b) without iso-surface

Figure 3.5: The local maximum points before drawing Liutex line

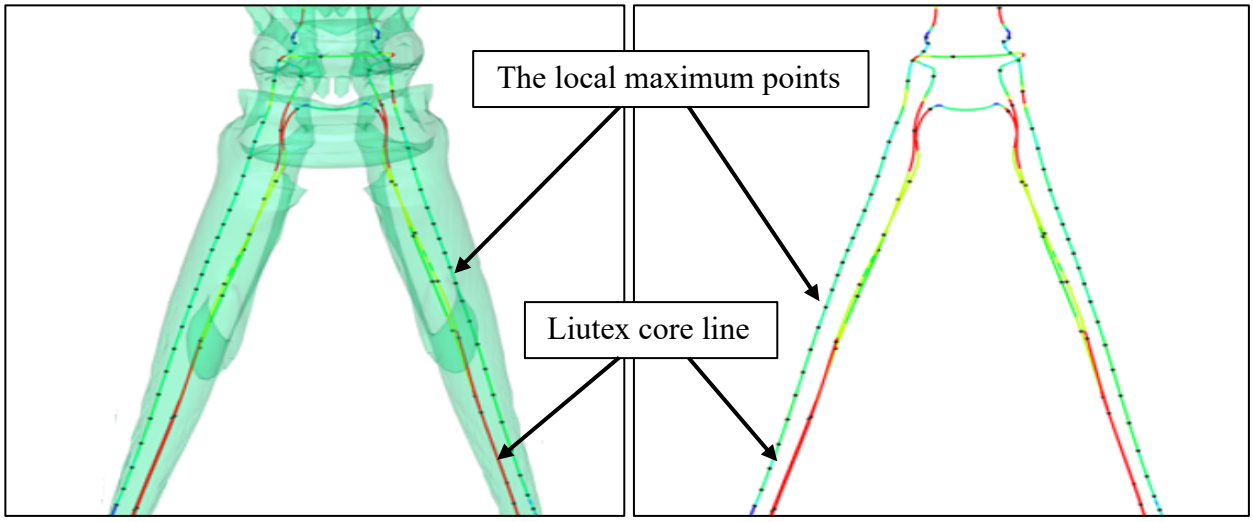

a) with iso-surface b) without iso-surface

Figure 3.6: The local maximum points after drawing Liutex line

Figure 3.7 and Figure 3.8 show the Liutex core line extracted for the early transition stage. The Liutex core line shows Λ-vortex structure the same as the modified Liutex-Omega iso-surface.

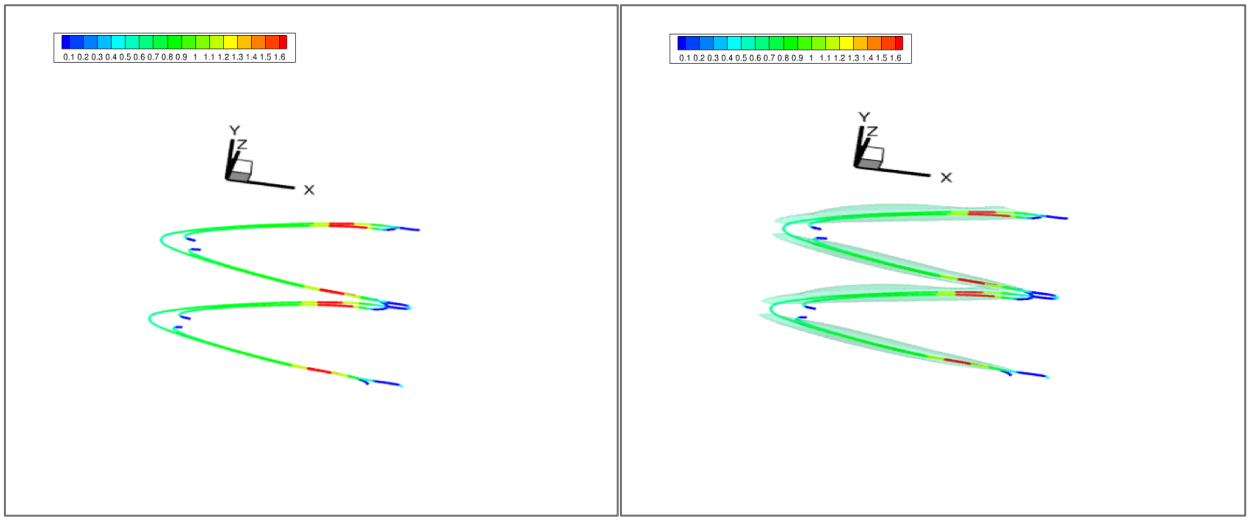

a) without iso-surface b) with iso-surface

Figure 3.7: The Liutex core line of Λ-vortex

While Figure 3.9 compares the Liutex core line with and without iso-surface for the late transition stage. The extracted Liutex core line succeeds in following the same vorticities structure as the modified Liutex-Omega iso-surface.

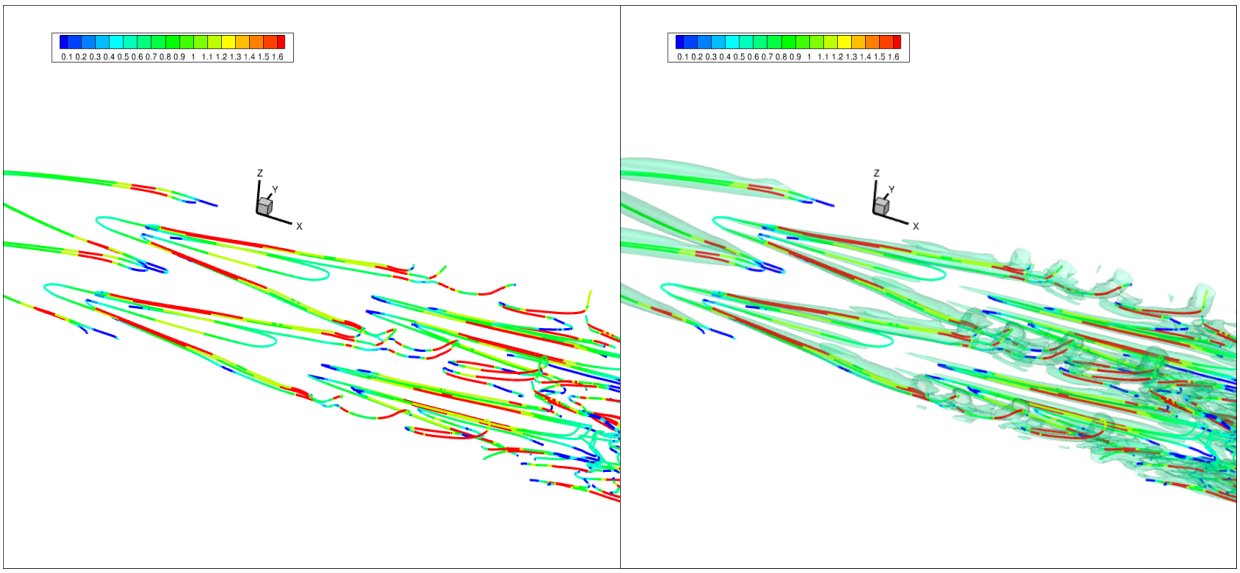

a) without iso-surface b) with iso-surface

Figure 3.8: A side view of the Liutex core line for early transition stage

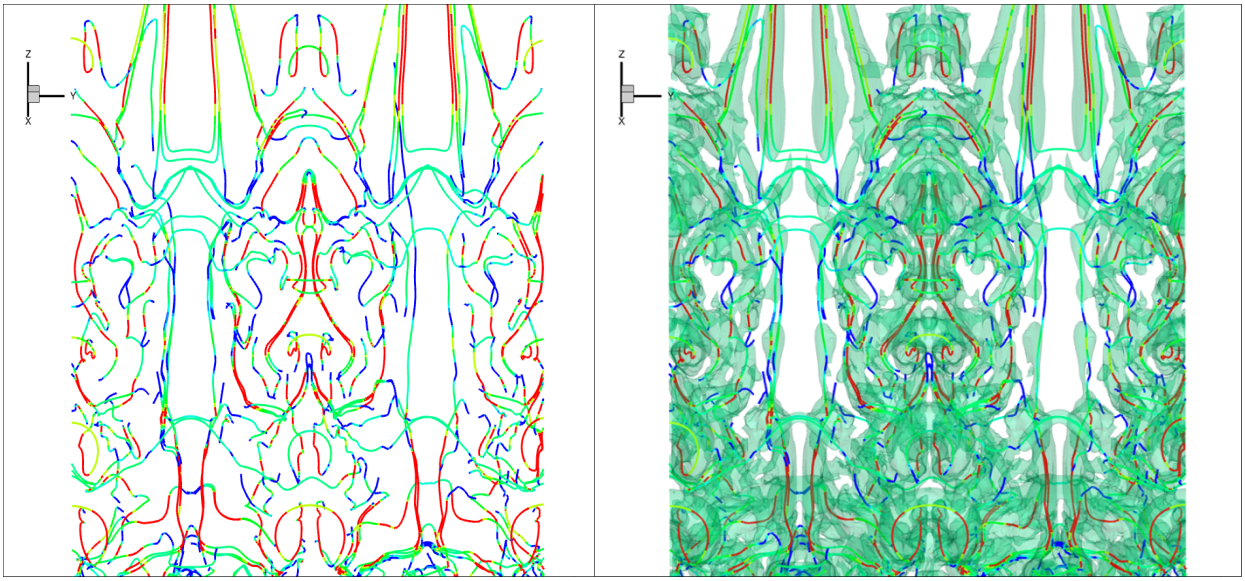

a) without iso-surface b) with iso-surface

Figure 3.9: A top view of the Liutex core line for late transition stage

Figure 3.10 and Figure 3.11 show top and side views of the Liutex core line for the very late transition stage. It may notice some noise in this late stage. Moreover, Figure 3.12 shows a top view of the Liutex core line of flow transition in boundary layers comparing with the iso-surface. The Liutex core line always follows the same structure as the modified Liutex-Omega iso-surface.

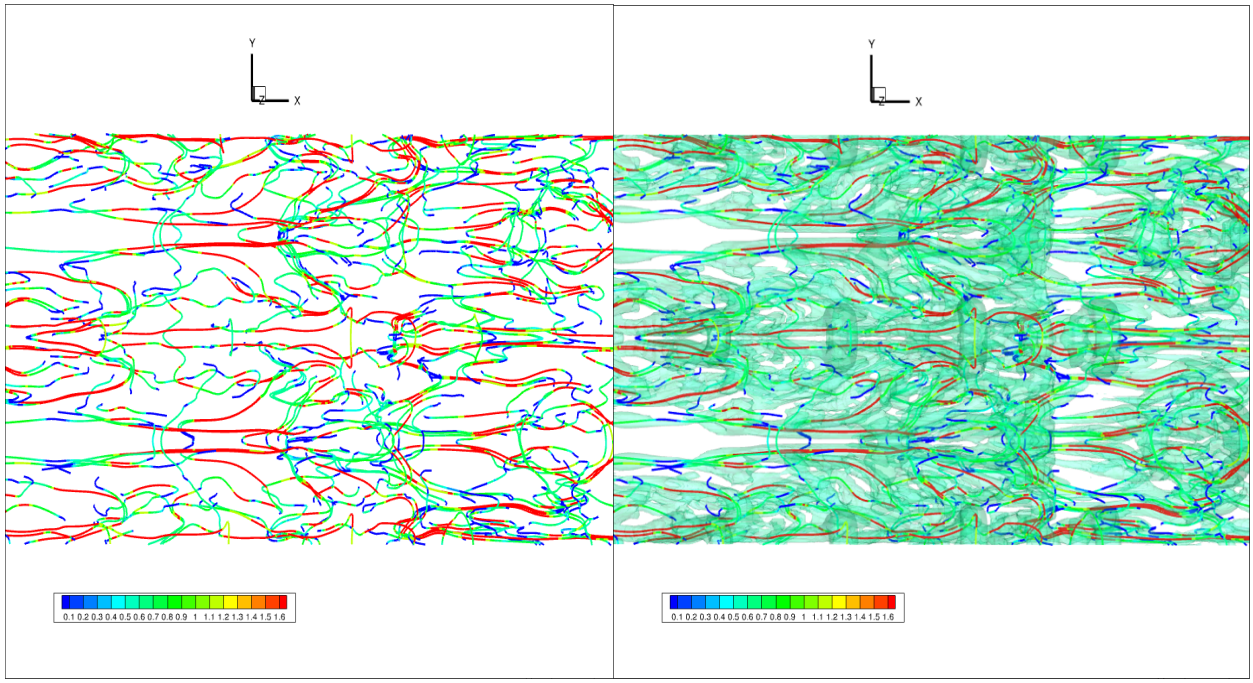

a) without iso-surface b) with iso-surface

Figure 3.10: A top view of the Liutex core line for the very late transition stage

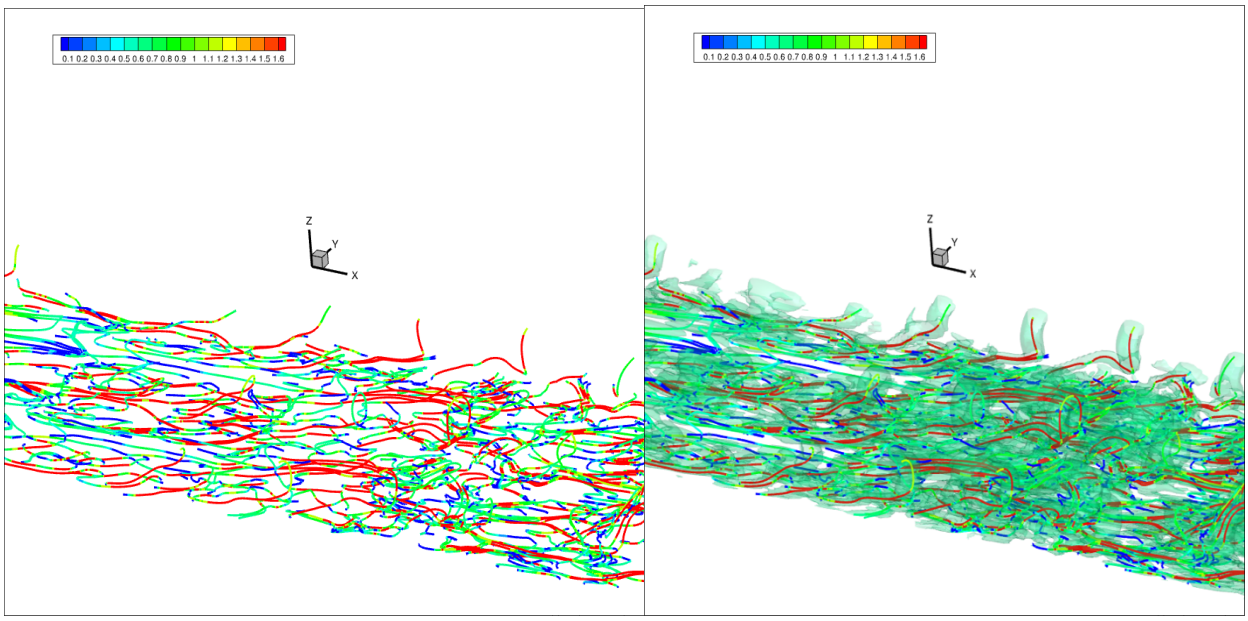

a) without iso-surface b) with iso-surface

Figure 3.11: A side view of the Liutex core line for the very late transition stage

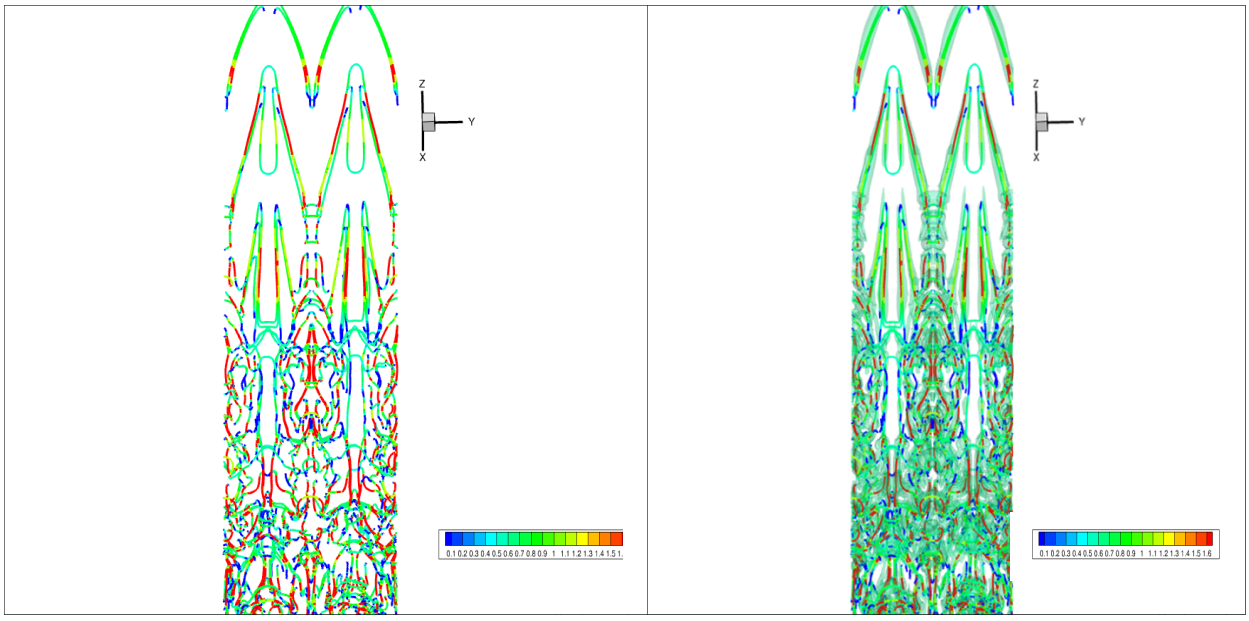

a) without iso-surface b) with iso-surface

Figure 3.12: A top view(zoom out) of the Liutex core line

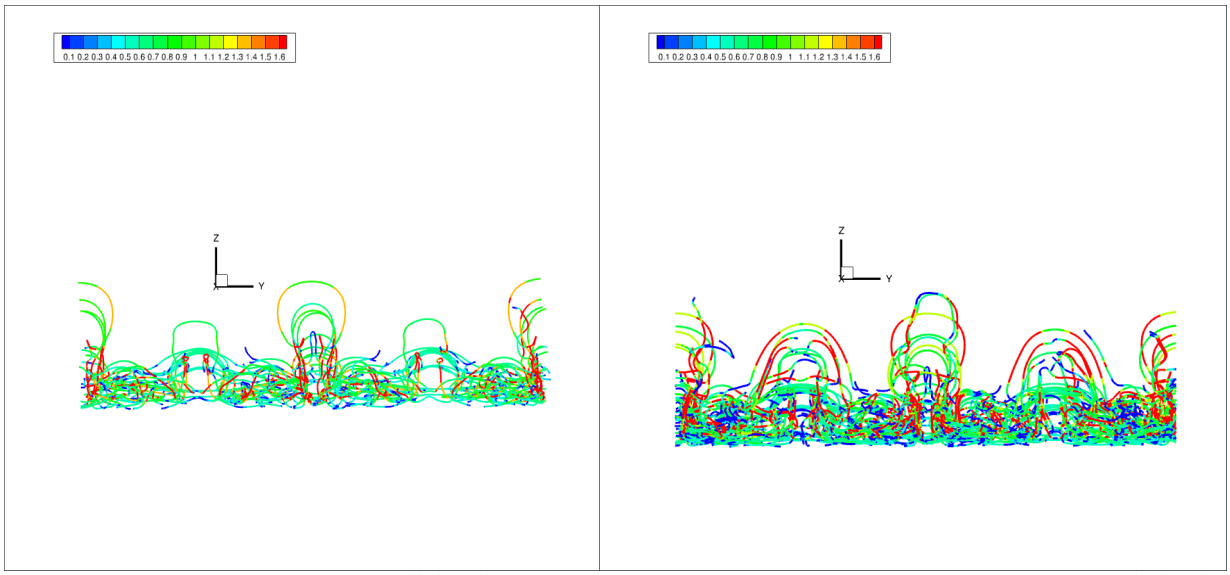

a)early transition stage b)late transition stage

Figure 3.13: A front view of the Liutex core line

The Liutex core line in the early transition stage shows the vortex structure clearly with almost no noises. However, in the late transition stage, when turbulence becomes stronger and vortices are severely curved, the noise appears little by little for several reasons. One of the reasons behind that is that the connection between the maximum points may be difficult due to the previously established coordinate grid, which may cause duplication of the Liutex line several times. Also, the numerical errors allow many fake maximum points to be calculated. Figure 3.14 shows that the Liutex core line structure has much noise and losing symmetry in the late transition stage.

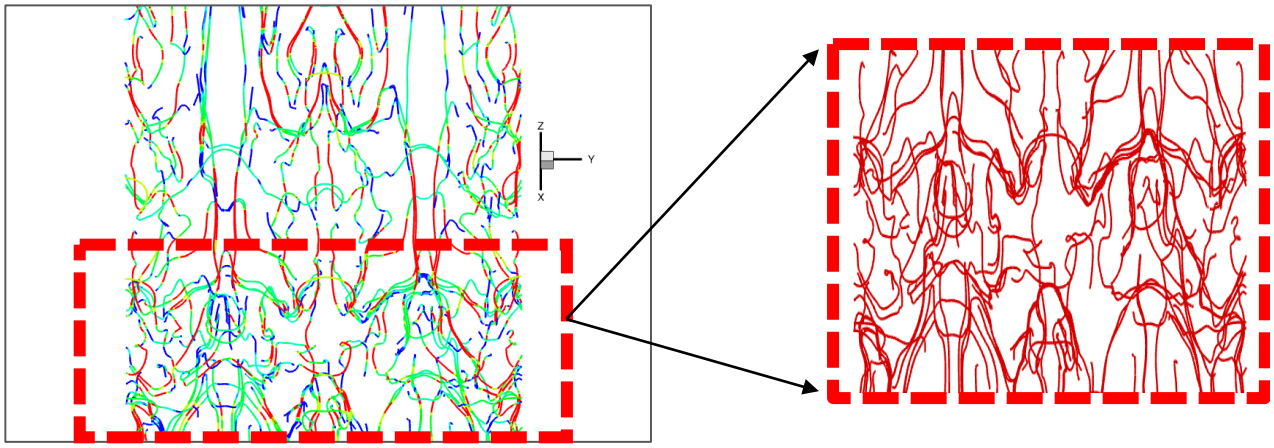

Figure 3.14: The Liutex core line structure with a lot of noise and losing symmetry in the late transition stage

3.5 The conclusion of the numerical results: Liutex core line method advantages

The Liutex core line method to visualize the vortex structure is the best vortex identification method for several reasons. The Liutex core line is the only method that gives a unique vortex structure, which is never affected by the threshold; see Figure 3.15 and Figure3.16. Unlike iso-surface-based methods, which produce an iso-surface structure, the Liutex core line has used the great benefit of Liutex to be a vector, so it is made of Liutex lines are defined everywhere. Also, the Liutex core line shows the strength of the vortex, and it can show the direction of the vortex as well, see Figure 3.17 and Figure 3.18.

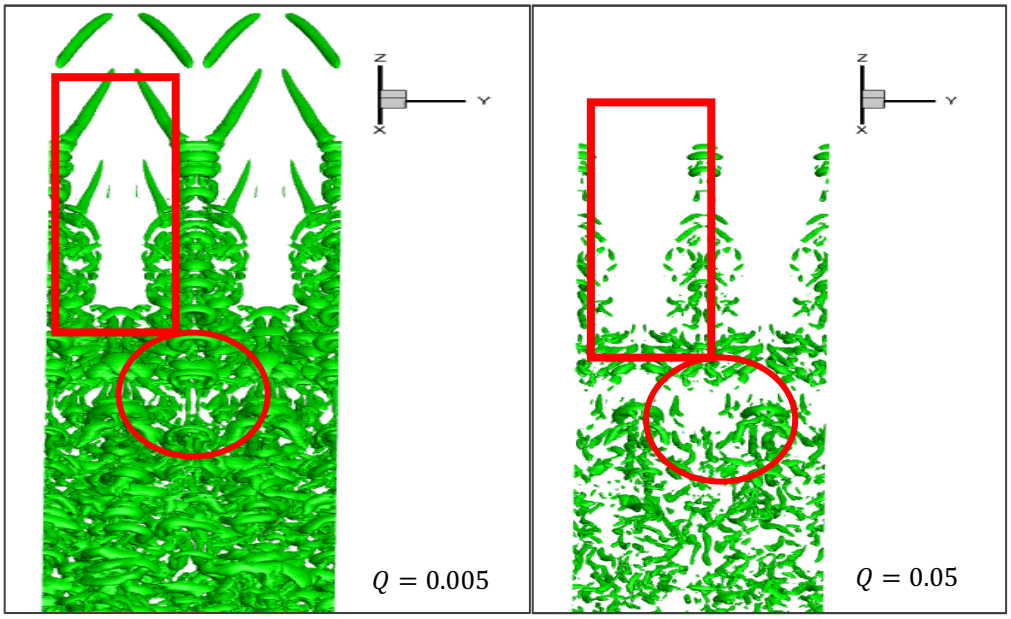

(a)Q-method with $Q = 0.005$ (b)Q-method with $Q = 0.05$

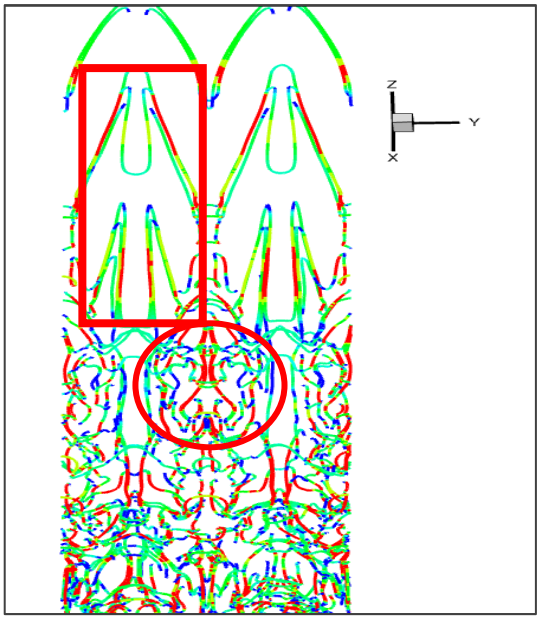

(c)Liutex Core Line never changes by threshold

Figure 3.15: Comparison between Q-method and Latex core line(zoom out)

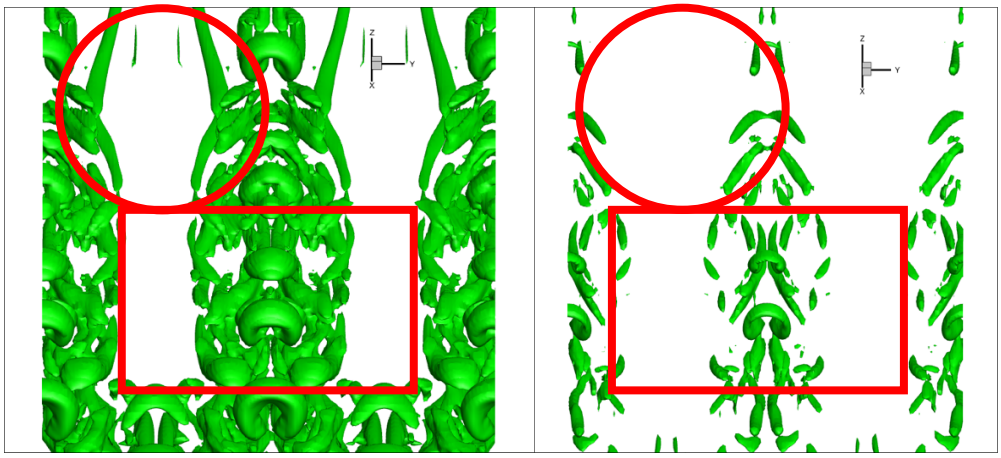

(a)Q-method with $Q = 0.005$ (b)Q-method with $Q = 0.05$

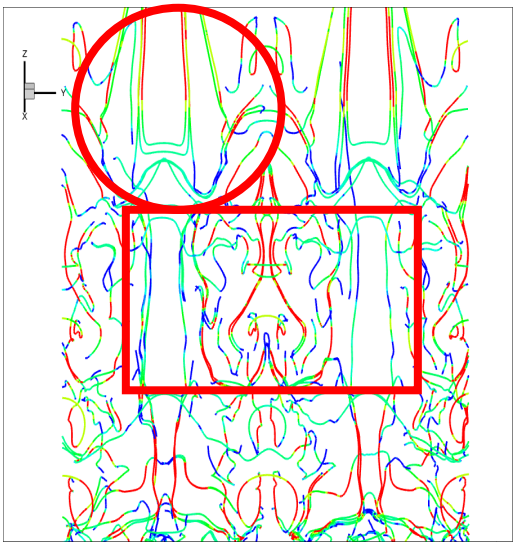

(c)Liutex Core Line never changes by threshold

Figure 3.16: Comparison between Q-method and Latex core line(zoom in)

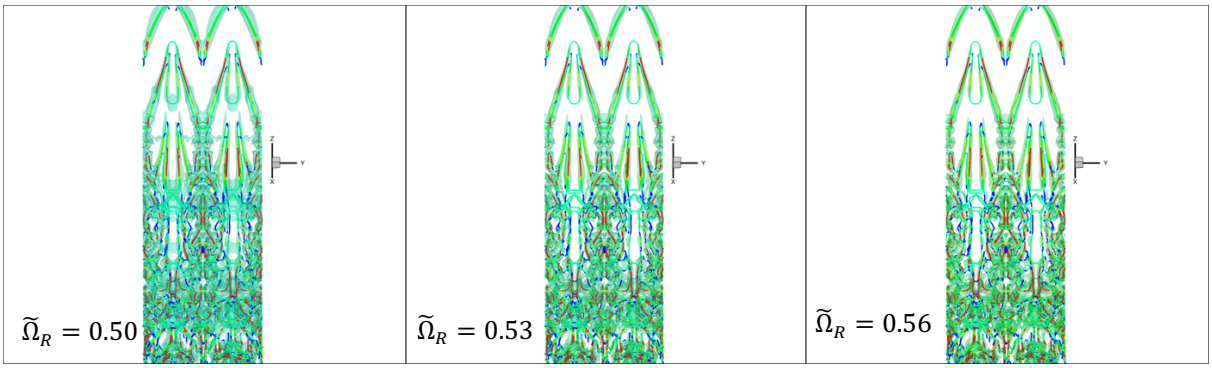
$\widetilde{\Omega}_R = 0.50$
$\widetilde{\Omega}_R = 0.53$
$\widetilde{\Omega}_R = 0.56$

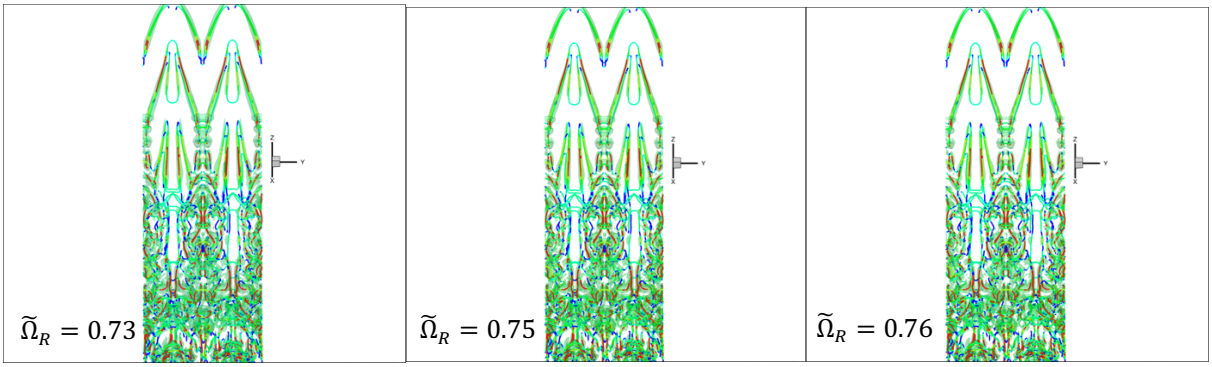
$\widetilde{\Omega}_R = 0.73$
$\widetilde{\Omega}_R = 0.75$
$\widetilde{\Omega}_R = 0.76$

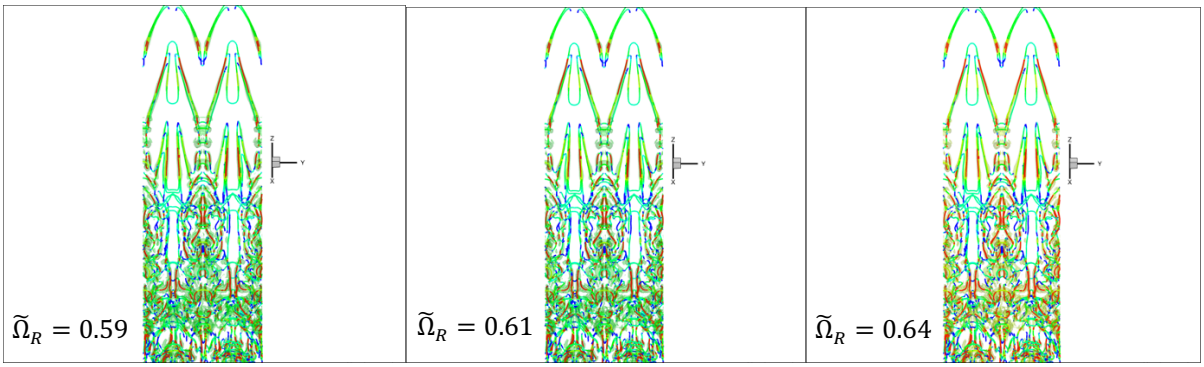
$\widetilde{\Omega}_R = 0.59$
$\widetilde{\Omega}_R = 0.61$
$\widetilde{\Omega}_R = 0.64$

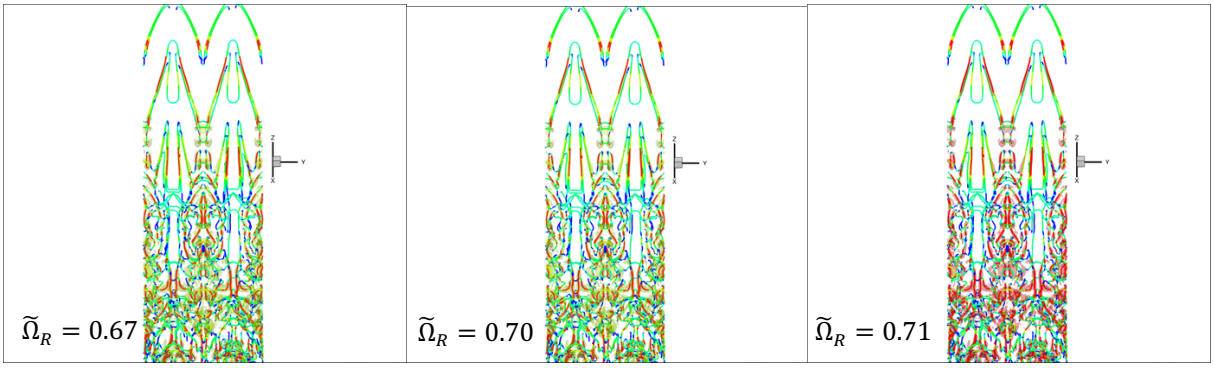
$\widetilde{\Omega}_R = 0.67$
$\widetilde{\Omega}_R = 0.70$
$\widetilde{\Omega}_R = 0.71$

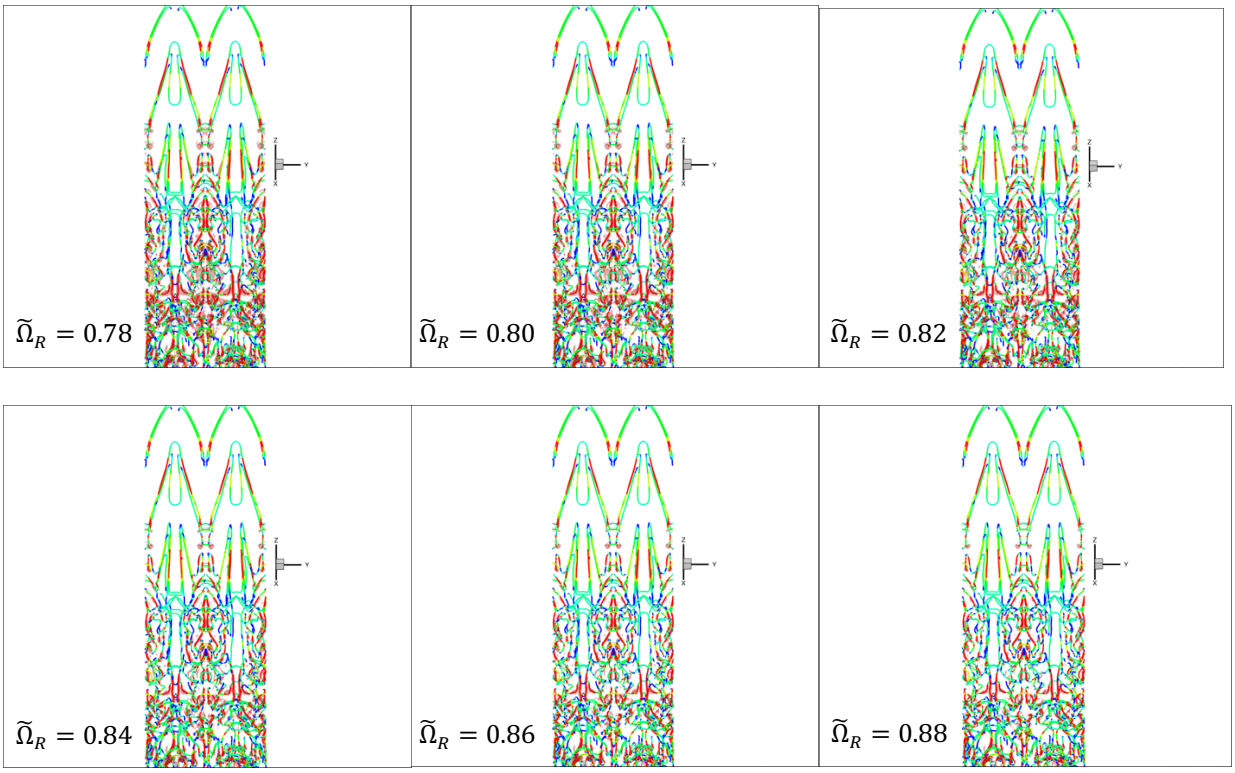

Figure 3.17: Proving the unique vortex structure of the Liutex core line, never changed in different thresholds

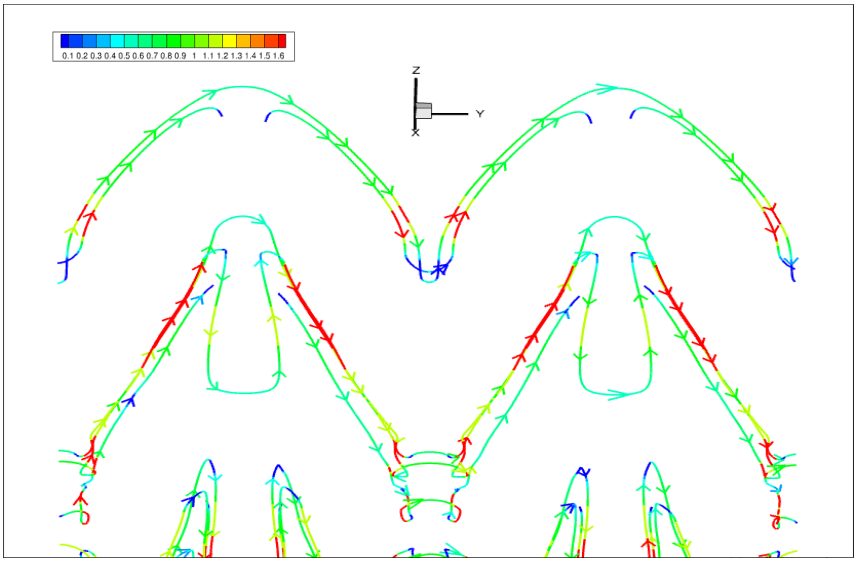

Figure 3.18: Liutex core line shows the direction of the fluid rotation axes

3.6 Summary:

This chapter intends to find the Liutex core line automatically. The differences between Liutex lines and vorticity lines have been discussed in the first section, which is found that Liutex lines can represent the vortex while the vorticity lines can not. The following sections, determining the local maxima points. The local maxima points have calculated by the second derivative test. These local maxima points have been filtered by apply the Liutex core line definition. The automatic method for finding the unique Liutex core line is the summarized section. Finally, the numerical result of applying this algorithm on the DNS data of flow transition in boundary layers is proposed.

CHAPTER 4

AN AUTOMATIC METHOD FOR FINDING A LIUTEX CORE TUBE

In this chapter, an automatic method to create a Liutex core tube to visualize the vortices structure will be shown. First, the manual method of finding a Linux core tube will discuss briefly to understand the idea of creating a tube out of Liutex lines. Then, an automatic method for finding Liutex core tube in detail will be proposed. The algorithm of the automatic method will be summarized in the following section. Finally, on the DNS data of flow transition in boundary layers, the numerical result of this automatic method will be shown in detail.

4.1 The manual method of Liutex Core tube

The vortex core line has an essential role in creating the vortex core tube since the core tube can be defined as the central area where fluid has a rotation, the area around the vortex core line. That means the vortex core tube structure depends on the vortex core line accuracy. In 2021, The manual method to find Liutex core tube using Liutex core line has been presented by Alvarez et al.[2]. In this section, Alvarez's manual method will be summarized to grasp the main idea of extract a tube using Liutex lines. See Chapter 2 and Chapter 3 for more information about Liutex lines. The DNS, early transition data of a flat plate, has been used in the original paper to construct the Liutex core line and Liutex core tube. It should be noted here that Alvarez used Liutex magnitude in his original paper. However, the researcher preferred to apply Alvarez's manual method on modified Liutex-Omega to obtain more precise and accurate figures.

4.1.1 Extract the Liutex core line manually:

First, pick a slice on the x-axis, which intersects with the leg of the hairpin vortex; see Figure 4.1. Near the intersection of the vortex region and the x-slice, take a sample of Liutex gradient lines. The Liutex gradient lines indicate the core line, which lets to locate the exact location of the Liutex core line.

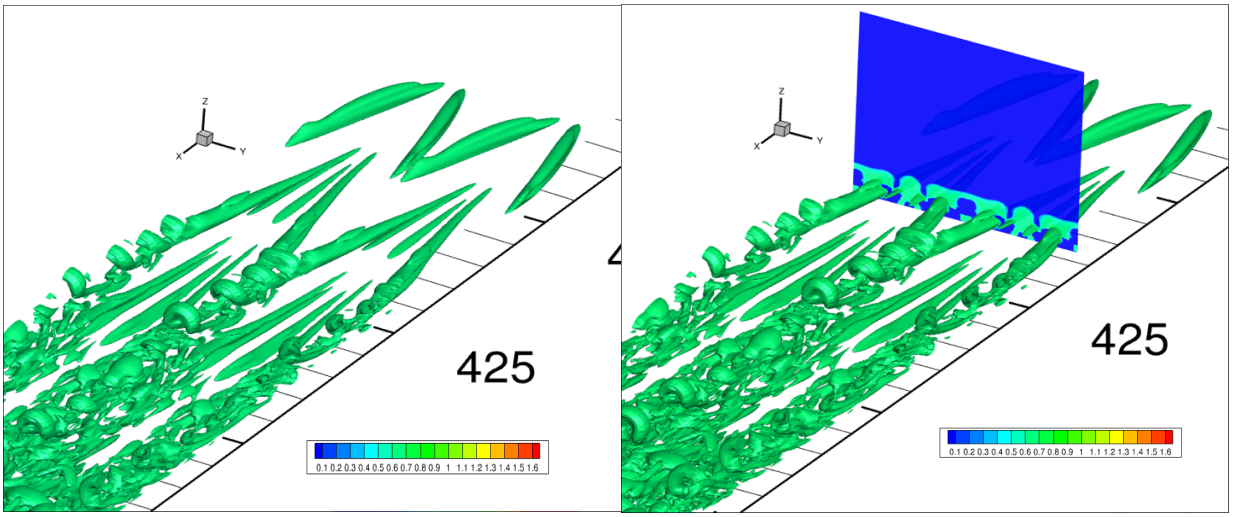

(a) $\widetilde{\Omega}_R = 0.52$ (b) X-slice at $X \approx 419$

Figure 4.1: DNS of the flat plate boundary layer with iso-surfaces drawn using Modified Liutex-Omega of 0.52 in the early transition phase

The intersection of the Liutex gradient lines and the X-slice exists at a local maximum point. Now, draw the Liutex core line, as in ref.[16], which pass through the intersection point of the Liutex gradient lines with the reference x-slice, the local maximum point. In Figure 4.2 and Figure 4.3, a Liutex line has been created at the intersection point.

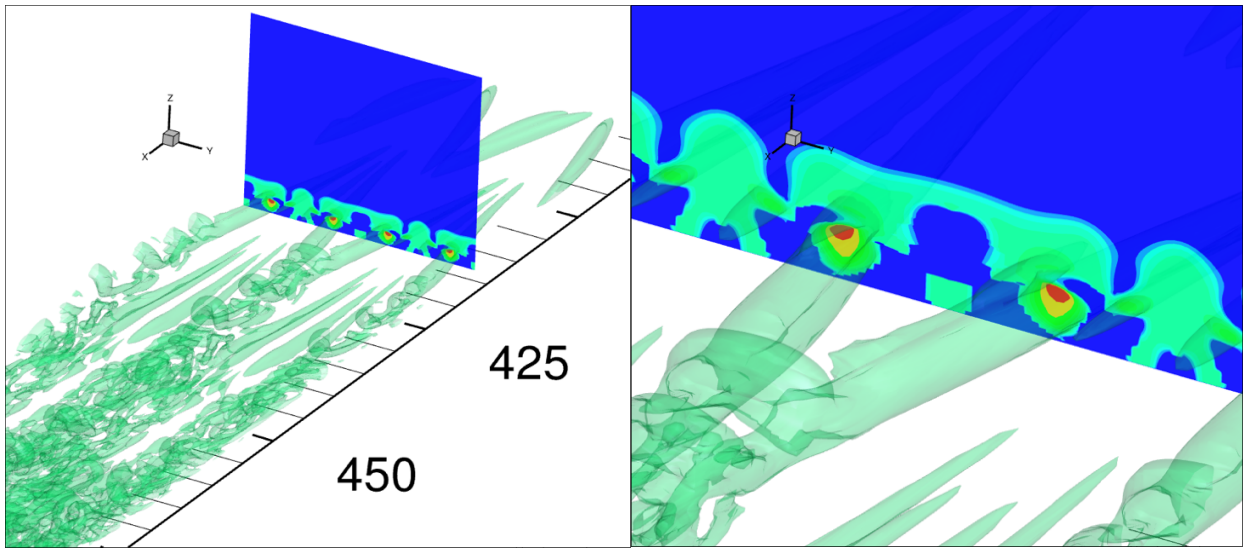

Figure 4.2: The intersection area of the iso-surface and the reference X-slice

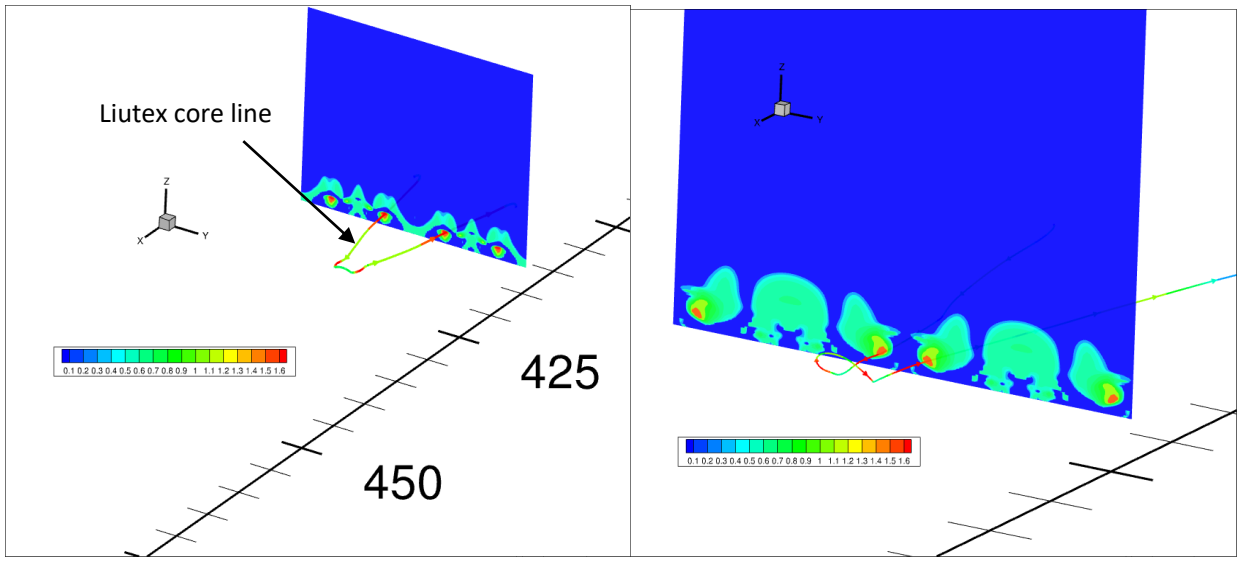

Figure 4.3.a: Liutex line drawn at the intersection point of the *X*-slice and Liutex gradient lines, which creates the Liutex core line without the iso-surface

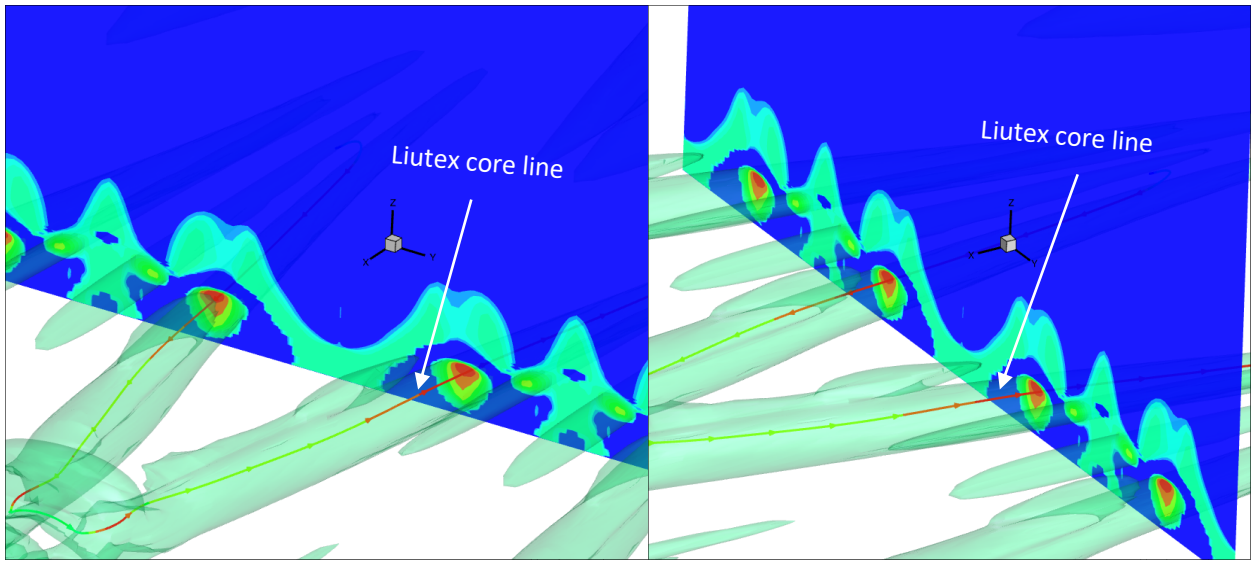

Figure 4.3.b: Liutex line drawn at the intersection point of the *X*-slice and Liutex gradient lines, which creates the Liutex core line with the iso-surface

4.1.2 Create a Liutex core tube manually:

Definition 4.1 The *Liutex Core Tube Magnitude Vector* is a vector lying on a plane that intersects with the Liutex core line were its initial point at the Liutex core line, the local maximum point, and its terminal point at an arbitrary percentage between 0 and 1.

So, the size of the tube can be decided via the Liutex core tube magnitude vector by chosen the percentage of terminal point, which is the length of this vector, see Figure 4.4.

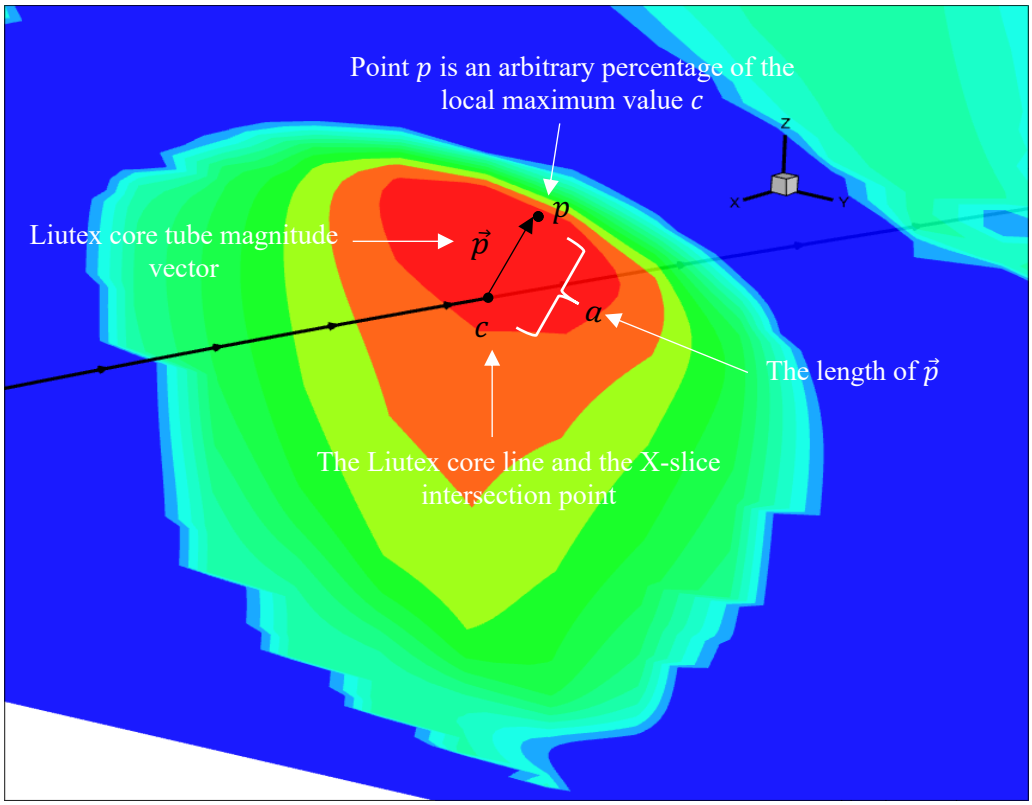

Figure 4.4: Liutex core tube magnitude vector p

In Figure 4.4, the point p is an arbitrary percentage of the local maximum point c where $0 < a < 1$. The condition that forces a to be between 0 and 1 is applied because of the following cases:

- If $a \leq 0$: so p is located where $\widetilde{\Omega}_R \leq 0.52$. That means there is no fluid rotation; in other words, there is no vortex anymore.
- If $a = 1$: so $p = c$, which means the Liutex core tube magnitude vector has a length of 0. That happens only at the local maximum point itself.
- If $a > 1$: that means there exist higher values than the local maximum point c, that is a contradiction of the existence of c.

After defining the Liutex core tube magnitude vector, plot Liutex lines through the terminal points around the Liutex core line to create the Liutex core tube; see Figure 4.5.

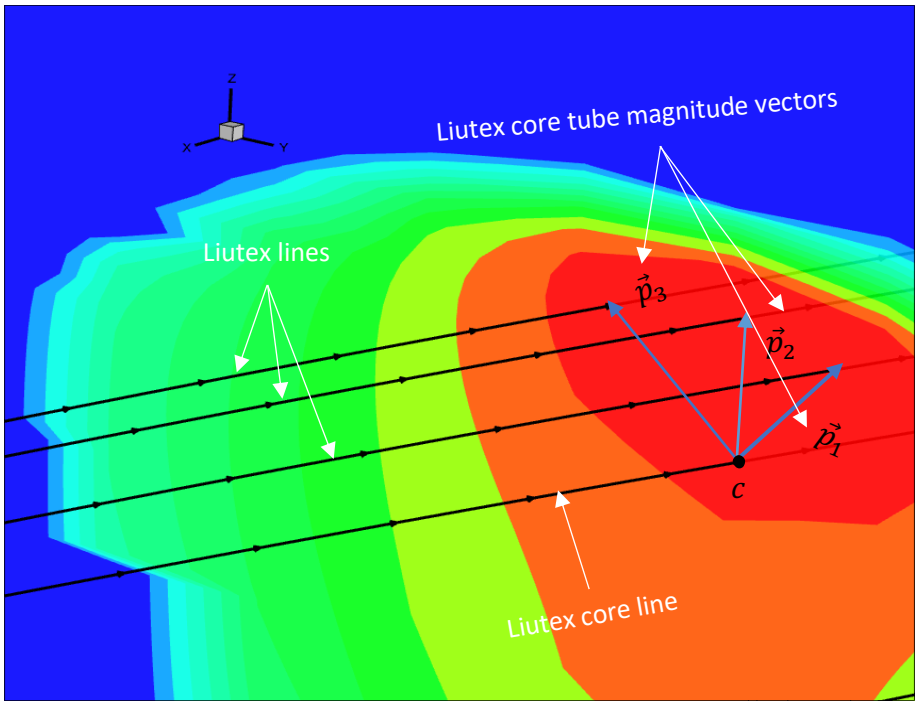

Figure 4.5: Liutex core tube magnitude vectors $\vec{p}_1$, $\vec{p}_2$, and $\vec{p}_3$

Then, the Liutex core tube is introduced as a collection of Liutex lines passed through some terminal points of a discrete or infinite amount of Liutex core tube magnitude vectors on a plane intersecting the Liutex core line. The manual method that is proposed by Alvarez et al. is successful; see Figure 4.6. However, in complex and severely curved vortices, the manual method of finding Liutex core tube seems not able to occur.

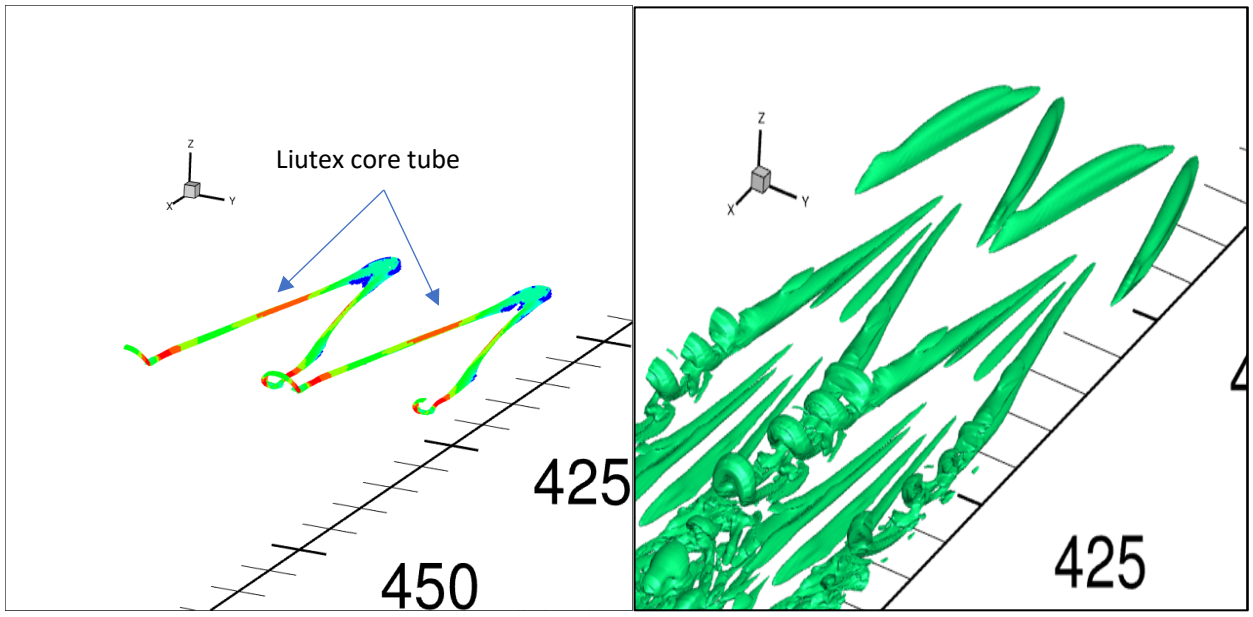

Figure 4.6: Liutex core tube creating manually by one local maximum point

In the next section, an algorithm to create a Liutex core tube will be proposed, dependent on the unique Liutex core line introduced in chapter 3. The importance of finding the Liutex tube is answering one of the significant issues, as stated in chapter 2, to identify any vortex, which is" What is the size of the vortex core?".

4.2 An automatic method for finding Liutex core tube

In this section, an algorithm to create a Liutex core tube will be presented, dependent on the unique Liutex core line introduced in chapter 3.

First, at every local maximum point found by algorithm 3.1, consider the X- slice, i.e., 2D-Plane (YZ-plane), as shown in Figure 4.7.

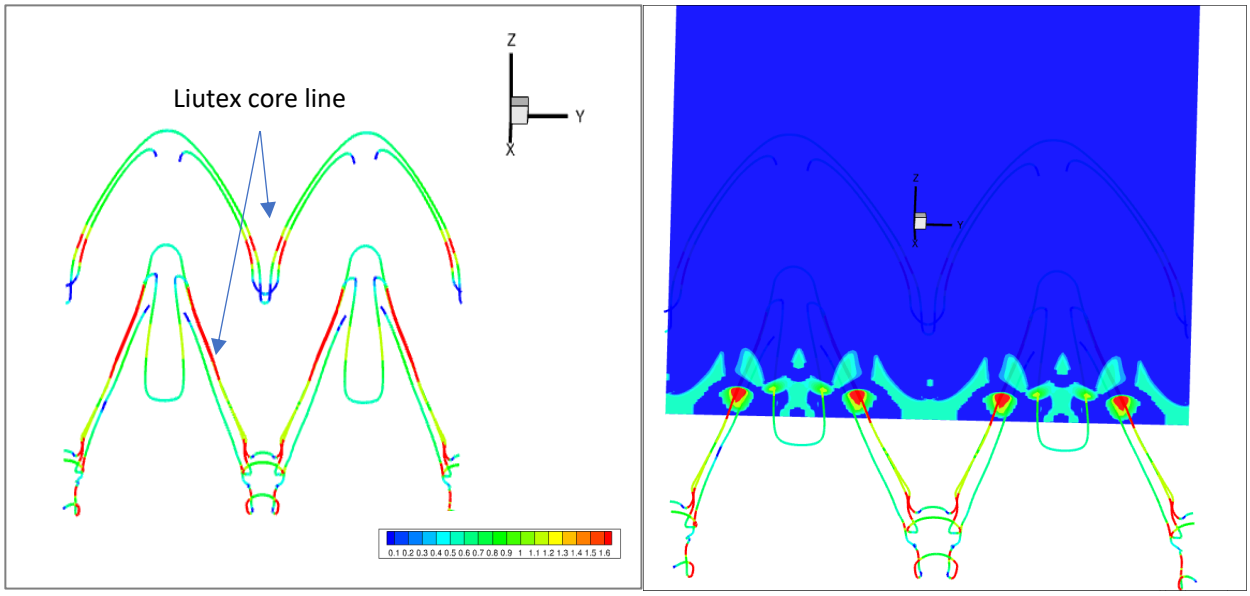

(a)without X-slice (b) with X-slice

Figure 4.7: Liutex core line creating by algorithm 3.1 in the early transition phase

So, if $p_0 = (x_0, y_0, z_0)$ is the intersection point between the Liutex core line and the reference X-slice, which is the local maximum point, then p_0 can be considered as $p_0 = (y_0, z_0)$ in the YZ-plane, the reference X-slice, see Figure 4.8.

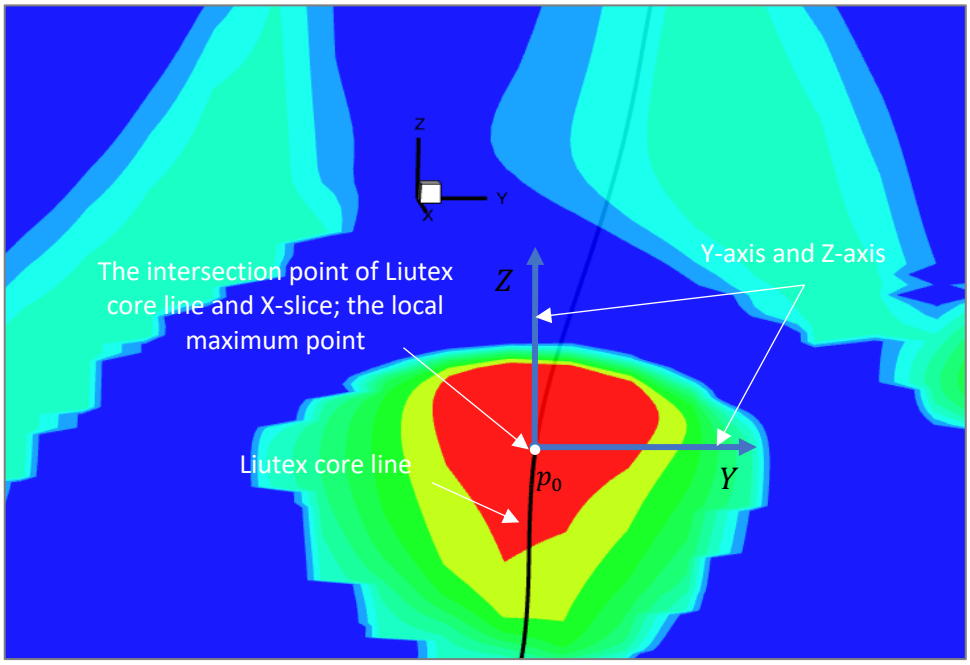

Figure 4.8: The intersection point of the Liutex core line and the reference X-slice; the local maximum point p_0

Now, the goal is finding finite or infinitely many points surrounding p_0 with a fixed distance; say a, of it. Notice that a represent the size of the tube and satisfies $0 < a < 1$. All these points satisfy the following equation.

$$(y - y_0)^2 + (z - z_0)^2 = a^2 \tag{4.1}$$

In Figure 4.9, it is easy to figure out the points $p_1 = (y_0 + a, z_0)$, $p_2 = (y_0, z_0 + a)$, $p_3 = (y_0 - a, z_0)$, and $p_4 = (y_0, z_0 - a)$. These points can be used as pre-conditions while equation (4.1) is solved to ensure that there are some points everywhere around p_0.

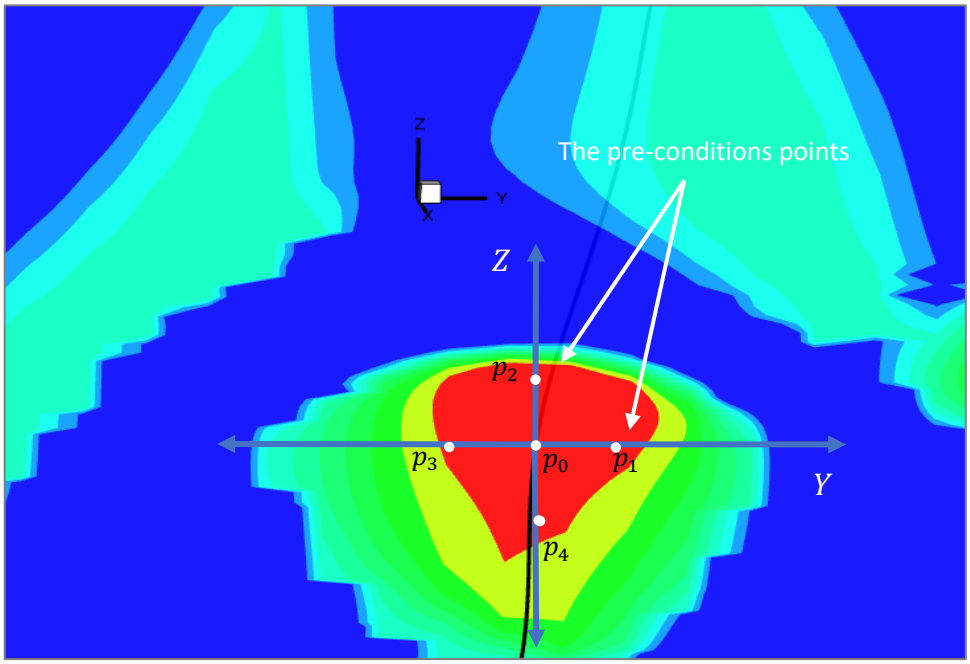

Figure 4.9: The pre-conditions points p_1, p_2, p_3, and p_4

After determining enough points surrounding p_0; see Figure 4.10, draw Liutex line through these new points to extract the Liutex core tube, see Figure 4.11.

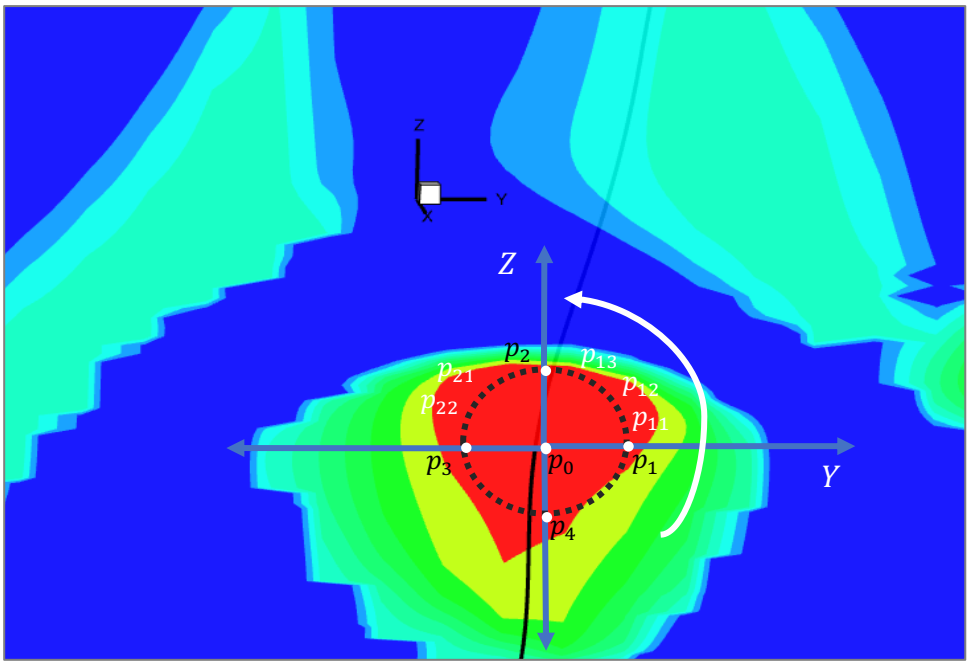

Figure 4.10: Determining the points that are between the pre-conditions points by solving (4.1)

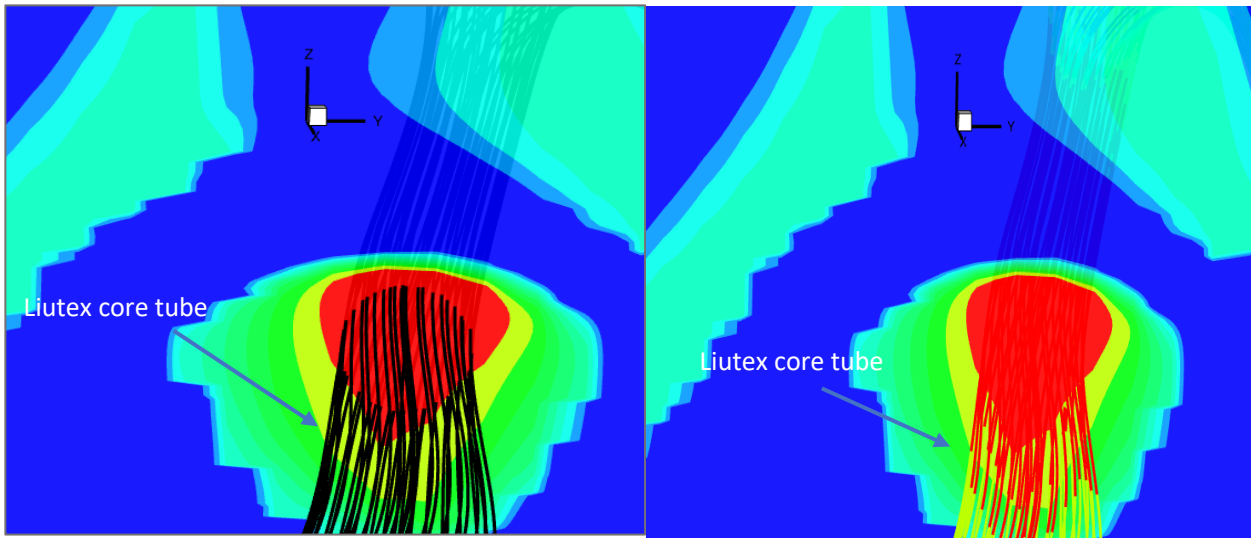

(a)Liutex core tube; black color (b)Liutex core tube; multi-color to show the strength

Figure 4.11: Liutex core tube with the reference X-slice

4.3 Algorithm of the automatic method for finding the Liutex core tube

In this section, an algorithm of extraction of a Liutex core tube automatically will be summarized as follows.

Algorithm 4.1: Finding a Liutex core tube

Rule 1: Consider a local maximum point, $p_0 = (x_0, y_0, z_0)$, that is obtained by Step 5 at algorithm 3.1, and select a value of a where $0 < a < 1$.

Rule 2: Calculate the following points:

$$\begin{cases} p_1 = (x_0, y_0 + a, z_0), \\ p_2 = (x_0, y_0, z_0 + a), \\ p_3 = (x_0, y_0 - a, z_0), \\ p_4 = (x_0, y_0, z_0 - a). \end{cases} \tag{4.2}$$

Rule 3: Solve the following problem:

$$\textit{Find } y \textit{ and } z \textit{ s.t.: } (y - y_0)^2 + (z - z_0)^2 = a^2 \tag{4.3}$$

In the following four cases:

Case1: $y_0 < y < y_0 + a$ and $z_0 < z < z_0 + a$

Case2: $y_0 - a < y < y_0$ and $z_0 < z < z_0 + a$

Case3: $y_0 - a < y < y_0$ and $z_0 - a < z < z_0$

Case4: $y_0 < y < y_0 + a$ and $z_0 - a < z < z_0$.

The output points have the form: $p_n = (x_0, y_n, z_n)$, for $n = 1,2,3,$ .... for each case.

Rule 4: Draw the Liutex lines through the new points that are obtained from the previous steps to extract the Liutex core tube.

Rule 5: Repeat the previous steps for all local maximum points that are obtained by Step 5 at algorithm 3.1.

It needs to highlight that problem (4.3) has infinitely many solutions. However, finding a finite number of solutions is enough in this case. To show that, let us consider the problem (4.3), solve it for z:

$$(z - z_0)^2 = -(y - y_0)^2 + a^2$$

$$z^2 - (2z_0)z = -y^2 + (2y_0)y + (a^2 - y_0^2 - z_0^2) \quad (4.4)$$

Assume it wants to find 50 different solutions. For case1, it is known that y belongs to the interval $(y_0,\ y_0 + a)$, so it is could be partition this interval into 50 equally spaces to know y values. By replace these values in (4.4), we get a quadratic equation with only one variable, z, which is so easy to solve, similarly for the rest cases.

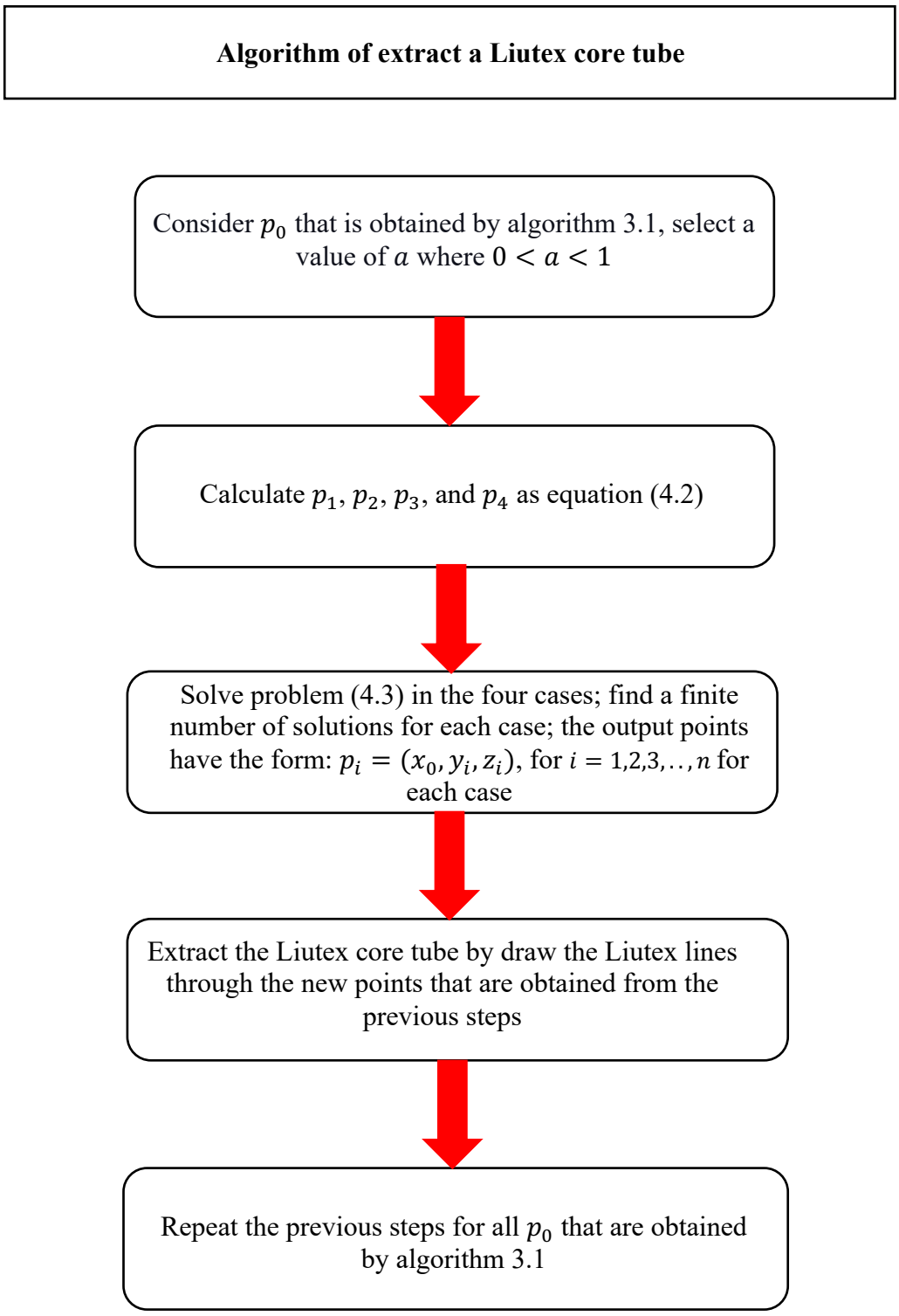

Figure 4.12: An algorithm of finding a Liutex core tube

4.4 The numerical result: testing case

In this section, the proposed automatic method is applied to find the Liutex core tube for the data obtained from a Direct Numerical Simulation (DNSUTA) of flow transition in boundary layers, which researchers from UTA and NASA Langley validated, see chapter 1.

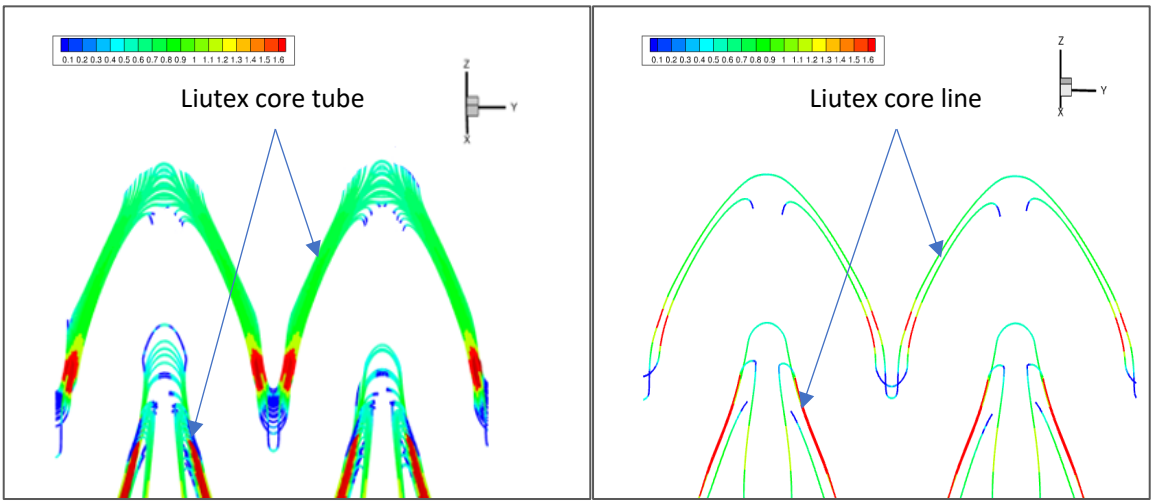

(a)Liutex core tube (b) Liutex core line

Figure 4.13: Liutex core tube and Liutex core line for early transition stage

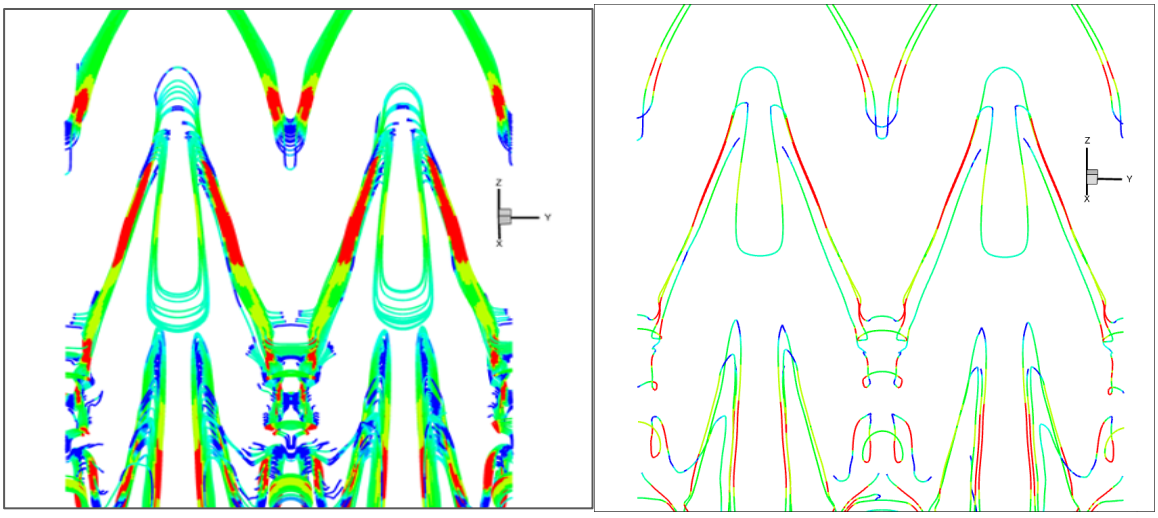

(a)Liutex core tube (b) Liutex core line

Figure 4.14: Liutex core tube and Liutex core line for the hairpin vortex

Figure 4.13 and Figure 4.14 show the Liutex core tube and Liutex core line, which were extracted, for the early transition stage. The Liutex core line shows the skeleton of the vortex, while the Liutex core tube shows the strength of the vortex clearly.

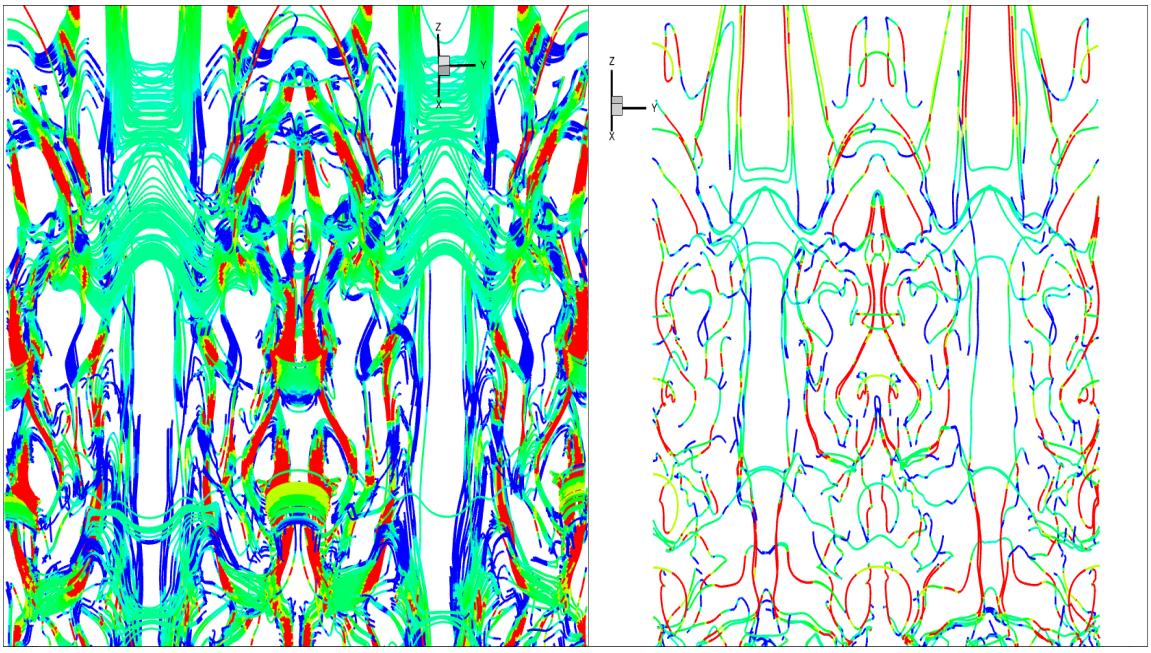

(a)Liutex core tube (b) Liutex core line

Figure 4.15: Liutex core tube and Liutex core line for late transition stage

Figure 4.15 compares the Liutex core tube and the Liutex core line for the late transition stage. The extracted Liutex core tube and Liutex core line always follow the same vorticities structure. While Figure 4.16 shows a top view of the Liutex core tube and the Liutex core line for the late transition stage. In the late stage, the noise may be noticed clearly. Moreover, Figure 4.17 shows a top view of the Liutex core tube of flow transition in boundary layers comparing with the Liutex core line for the same snapshot.

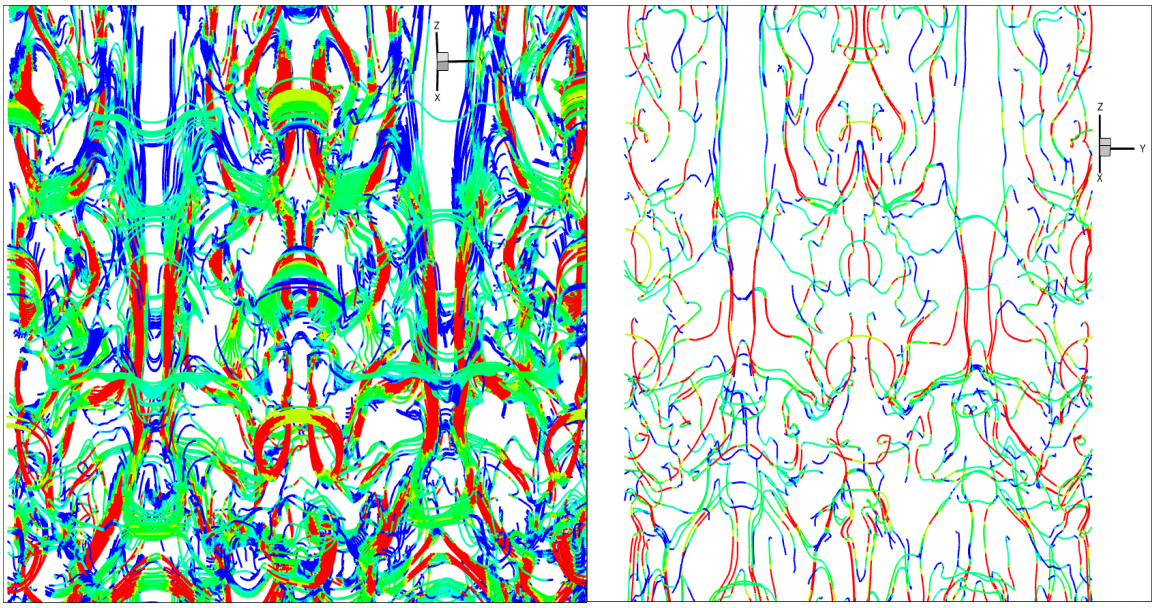

(a)Liutex core tube (b) Liutex core line

Figure 4.16: Liutex core tube and Liutex core line for very late transition stage

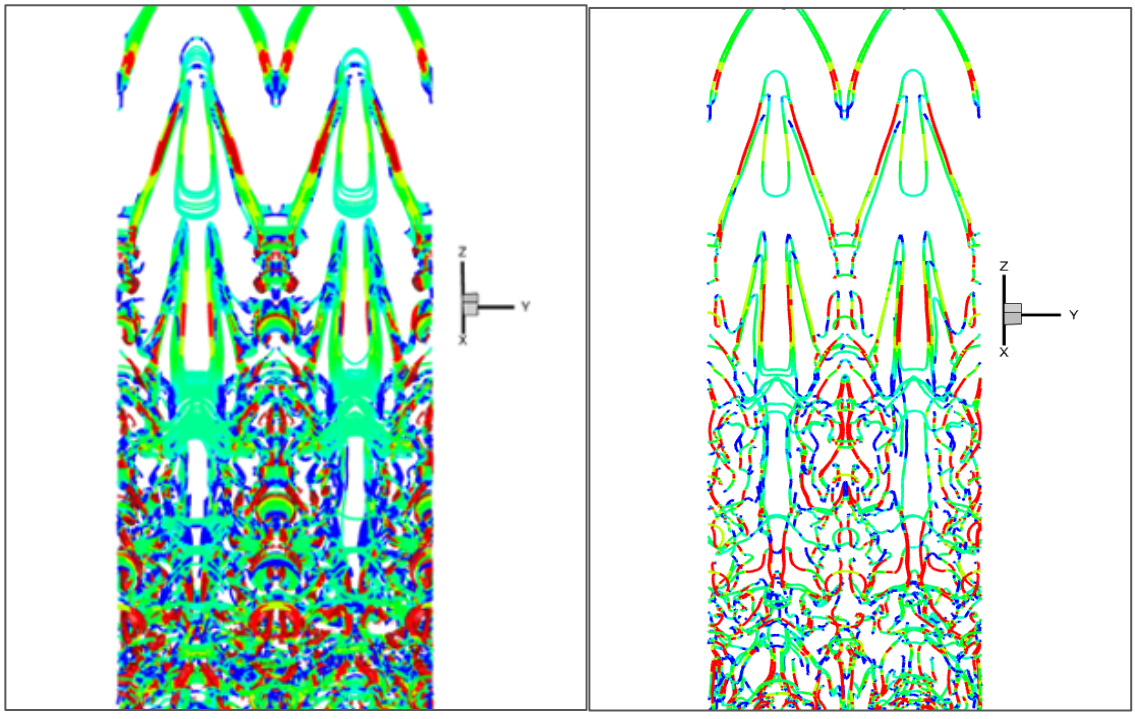

(a)Liutex core tube (b) Liutex core line

Figure 4.17: A top view(zoom out) of Liutex core tube and Liutex core line

Like the Liutex core line, the Liutex core tube in the early transition stage clearly shows the vortex structure with almost no noises. However, in the late transition stage, when turbulence becomes stronger, and vortices are severely curved, the noise appears little by little for the same reasons stated in Chapter 3.

4.5 The conclusion of the numerical results: Liutex core tube method advantages

Even though the Liutex core tube is never affected by the threshold, the Liutex core tube is not unique. The reason behind that is back to the size which is setting by the user. However, one of the advantages of the Latex core tube is showing the strength of the vortices structure very clearly, unlike the iso-surface methods, see Figure 4.18. Besides showing some size of the vortex structure, the Liutex core tube can show the vortex direction like the Liutex core line because both are made by Liutex lines. Figure 4.19 shows the direction of the vortex.

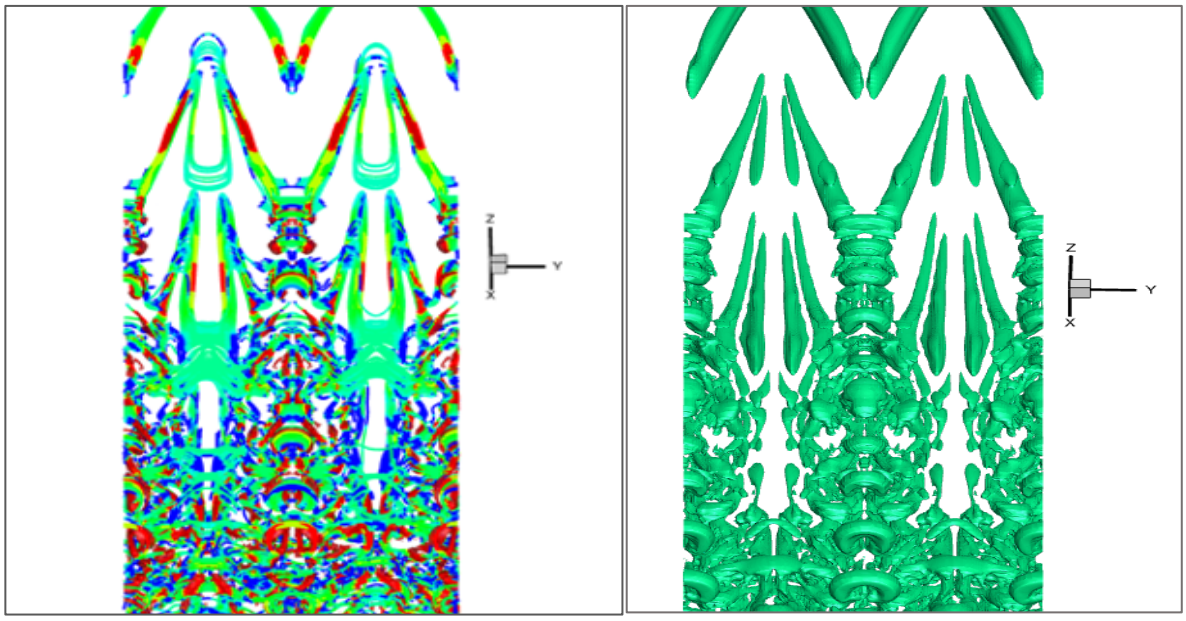

(a)Liutex core tube (b) the iso-surface of $\widetilde{\Omega}_R = 0.52$

Figure 4.18: Comparison between Liutex core tube and the iso-surface where the iso-surface never shows any strength of the vortex

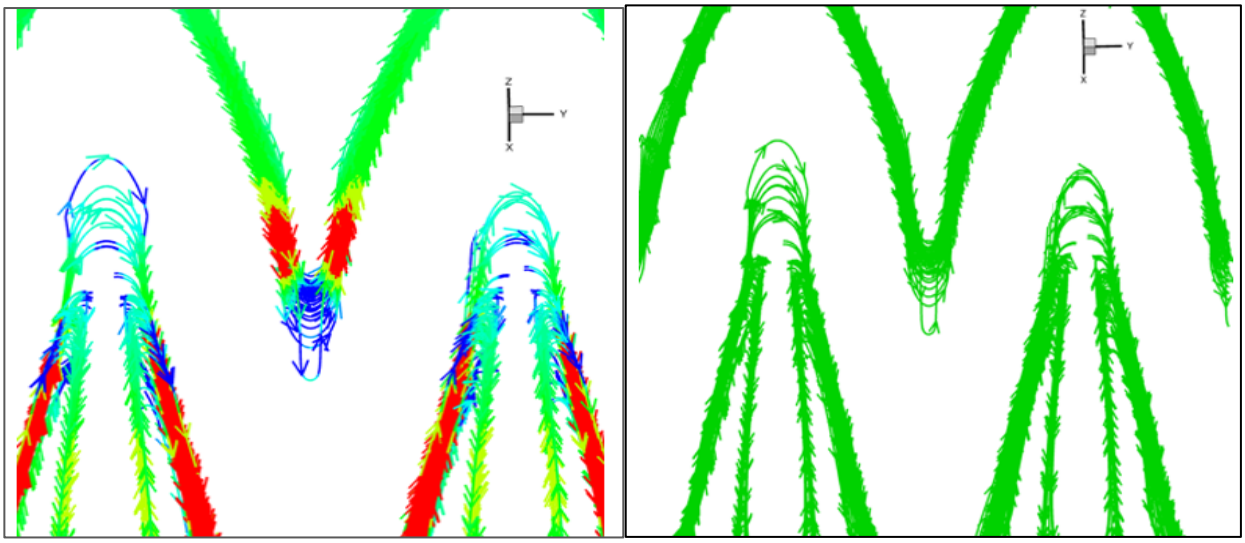

(a) Multi-color (b) One color (Green)

Figure 4.19: Liutex core tube shows the direction of the vortex

4.6 Summary:

In this chapter, the main goal is to find the Liutex core tube automatically. The manual method of finding the Liutex core tube has discussed in the first section. The result of the manual method is successful. However, creating a Liutex core tube for complex and severely curved vortices is difficult. In the following section, an automatic method for finding Liutex core tube has proposed in detail. Since the Liutex core tube depends on the Liutex core line, the automatic method started from the local maximum points obtained by algorithm 3.1. Finally, the numerical result of applying this automatic method on the DNS data of flow transition in boundary layers is presented.

CHAPTER 5

CONCLUSIONS AND FUTURE STUDIES

Liutex and related Liutex methods (Ω_R and $\widetilde{\Omega}_R$) excel the first and second generations of vortex identification methods. Liutex method can be defined as the rotation part of fluid motion. Liutex method also provides a vector, scalar, and tensor forms. So it has been efficiently used to identify the vortex structures in this study and extract the Liutex core line and tube. In this study, the answer to two essential issues of vortex definition and identification has presented: (1) What is the rotation axis? (2) What is the size of the vortex core? An algorithm to locate the Liutex core line has been introduced in chapter 3. While an algorithm to find a Liutex core tube has been presented in chapter 4. In this dissertation, the researcher uses the modified Liutex-Omega to extract the points because it can capture both weak and strong vortex at the same time. The data obtained from a Direct Numerical Simulation (DNSUTA) of flow transition in boundary layers, which researchers from UTA and NASA Langley validated, has been used to show the result in this dissertation.

Liutex lines have compared with vorticity lines, and it turns out that vorticity lines cannot identify the vortex, unlike Liutex lines. The automatic method of finding the Liutex core line is started by setting the threshold of the modified Liutex-Omega to be $\widetilde{\Omega}_R = 0.52$. Finding the local maxima points using the second derivative test was the second step. Liutex core line definition: $\nabla R \times \vec{r} = 0$ has been applied after that with the convective derivative decomposition that is proposed by Wang [42]. has been applied after that with the convective derivative decomposition proposed by Wang [42]. The automatic method for finding the unique Liutex core line has summarized in the next section. The numerical results have shown after applying the previously

presented algorithm. It can be concluded that the Liutex core line method is the best method to visualize the vortex structure for three reasons: (1) It is unique, (2) showing the strength, and (3) showing the direction of the rotation axis.

The manual method of creating a Liutex core tube has introduced using the modified Liutex-Omega instead of Liutex magnitude in the original paper. The manual method starts by extracting the Liutex core line manually, then Creates a Liutex core tube after selecting the tube size, a value between 0 and 1, by the user. The manual method that is proposed that proposed in Chapter 4 [2] seems a successful method, but adopting this method is impossible in complex and severely curved vortices. Hence the need to find an algorithm that presents a Liutex core tube. An algorithm to create a Liutex core tube has been presented after depending on the unique Liutex core line, which is introduced in Chapter 3. The algorithm of the automatic method for finding the Latex core tube has been summarized next. After applying the previously presented algorithm, the numerical results have shown in the next section. As a conclusion of the Liutex core tube method to visualize the vortex structure, it can be point the following:(1) Liutex core tube is not unique because the different choice of a value produces different tube with different size. However, the Liutex core tube is unique concerning the threshold because it is not affected by changing the threshold since it is made of Liutex lines. (2)Liutex core tube is the only method of vortex identification method that shows the vortex size. (3) Like the Liutex core line, the Liutex core tube shows the strength and the direction of the vortex.

In this dissertation, two essential issues of the vortex identification method are addressed in detail. The first issue is: What is the rotation axis? In chapter 3 the researcher has provided an algorithm of the Liutex core line based on clear and reasonable mathematical explanations to answer the first issue. The second issue is: What is the size of the vortex core? Chapter 4 has

been presented an algorithm to answer this issue as well. The importance of both the Liutex core line and Liutex core tube is that they are not affected by changing of the threshold, unlike the previous methods of the first, second, and third, such as Liutex, Liutex-Omega as they all are iso-surface identification methods presentations. So, they are affected by the threshold changing. depending on the intensity of the In the late transition stage, the noise appears little by little depending on the intensity of the turbulence, and vortices strength. there are many reasons such as the previously established coordinate grid that caused some difficulty in the connection between the maximum points. the other reason is the numerical errors, which permit a lot of fake maximum points to be calculated. As future studies, it may be suggested to study these problems deeply and solve them. as an improvement the established coordinate grid and reduce the numerical errors values.

Table 5.1 presents a comparison between some vortex identification methods, which shows the superiority of the Liutex core line method on others. Since the Liutex core Line method is free of threshold and produces a unique vortex structure, the Liutex core line method is the best vortex identification method so far.

Table 5.1: Comparison between some vortex identification methods

	The method name	iso-surface structure	Threshold	Uniqueness	show vortex strength	show vortex direction
Second Generation	Q-method	Yes	Very sensitive	No	No	No
	λ_2-method	Yes	Very sensitive	No	No	No
Third Generation	Liutex iso-surface	Yes	Sensitive	No	No	No
	Modified Liutex Omega	Yes	Insensitive	No	No	No
	Liutex core line	No	No needed	Yes	Yes	Yes
	Liutex core tube	No	No needed	No	Yes	Yes

REFERENCES

[1] Abdel-Raouf, E., Sharif, M.A., and Baker, J., "Impulsively started, steady and pulsated annular inflows," Fluid Dynamics Research, Vol. 49, No. 2, 2017, Article ID 025511.

[2] Alvarez et al., "Visualizing Liutex core using Liutex lines and tubes." Liutex and Third Generation of Vortex Definition and Identification: An Invited Workshop from Chaos 2020, ISBN-10 : 3030702162, Springer, 2021. https://www.springer.com/gp/book/9783030702168

[3] Amara, D. K, "How To Escape From Falling Into The Saddle Points On A Non-Convex Surface Various Types of Critical Points.", 2019, DOI:10.13140/RG.2.2.19423.41129, https://www.researchgate.net/publication/335946506

[4] Bake, S., Meyer, D., and Rist, U., "Turbulence mechanism in Klebanoff transition: a quantitative comparison of experiment and direct numerical simulation," J. Fluid Mech., Vol. 459, 2002, pp. 217-243.

[5] Banks D. C., Singer B. A., "Vortex tubes in turbulent flows: Identication, representation, reconstruction," *Proceedings of the Conference on Visualization '94*, Los Alamitos, CA, USA, 1994.

[6] Chen, L., and Liu, C., "Numerical study on mechanisms of second sweep and positive spikes in transitional flow on a flat plate," J. Comput. Fluids, Vol.40, 2011, pp. 28–41.

[7] Chong, M. S. et al. "A general classification of three-dimensional flow fields." Phys. Fluids A 2, 1990, 765–777

[8] Dong, X., Tian, S., and Liu, C. "Correlation analysis on volume vorticity and vortex in late boundary layer transition," Physics of Fluids , Vol. 30, No. 1, 2018, Article ID 014105.

[9] Dong, X., Wang, Y., Chen, X., Dong, Y., Zhang, Y., and Liu, C., "Determination of epsilon for Omega vortex identification method," Journal of Hydrodynamics, Vol. 30, 2018, pp. 541-548.

[10] Dong, Y., Yang, Y., and Liu, C., "DNS Study on Three Vortex Identification Methods," AIAA paper 2017-0137, January 2017.

[11] Dong, Y., Yan, Y. & Liu, C., "New visualization method for vortex structure in turbulence by lambda2 and vortex filaments," Applied Mathematical Modelling, Volume 40, Issue 1, 2016, Pages 500-509, ISSN 0307-904X, https://doi.org/10.1016/j.apm.2015.04.059.

[12] Epps, B., "Review of Vortex Identification Methods," AIAA paper 2017-0989, January 2017.

[13] Gao Y., Liu C., “Rortex and comparison with eigenvalue based vortex identification criteria,” *Physics of Fluids*, 2018, 30: 085107.

[14] Gao Y., Liu J., Yu Y. et al., “A Liutex based definition and identification of vortex core center lines,” *Journal of Hydrodynamics*, 2019, 31(2): 774-781.

[15] Gao, Y., and Liu, C., “Rortex based velocity gradient tensor decomposition,” Physics of Fluids, 2019, 31(1): 011704.

[16] Gao, Y., Liu, J., Yu, Y., and Liu, C., “A Liutex based definition and identification of vortex core center lines,” Journal of Hydrodynamics, 2019, Vol. 31(3), pp. 445-454.

[17] Hänninen, Risto., Baggaley, Andrew W., “Vortex filament method as a tool for computational visualization of quantum turbulence,” Proceedings of the National Academy of Sciences, 2014, 111 (Supplement 1) 4667-4674; DOI: 10.1073/pnas.1312535111 https://doi.org/10.1073/pnas.1312535111

[18] Helmholtz H., “Über Integrale der hydrodynamischen Gleichungen, welche den Wirbelbewegungen entsprechen,” *Journal für die reine und angewandte Mathematik*, 1858, 55: 25-55.

[19] Herman, E. J., Strang, G. “Calculus Volume 1. ” , 2018 Rice University. https://d3bxy9euw4e147.cloudfront.net/oscms-prodcms/media/documents/calculus-volume-1-5.2-previous.pdf

[20] Hunt J. C. R., Wray A. A., Moin P., “Eddies, stream, and convergence zones in turbulent flows,” [R]. Center for Turbulent Research Report CTR-S88, 1988, 193-208.

[21] Jeong J., Hussain F., “On the identification of a vortex,” [J]. *Journal of Fluid Mechanics*, 1995, 285: 69-94.

[22] Keisler, H. J, “Elementary Calculus: An Infinitesimal Approach.” , 2000, On-line Edition, http://www.math.wisc.edu/~keisler/calc.html

[23] Kida S., Miura H., “Identification and analysis of vertical structures,” *European Journal of Mechanics-B/Fluids*, 1998, 17(4): 471-488.

[24] Kivotides D, Barenghi CF, Samuels DC, “Triple vortex ring structure in superfluid helium.” , 2000, Science 290(5492):777-779.

[25] Lee, C. B., and Li, R. Q., “A dominant structure in turbulent production of boundary layer transition,” J. Turbul., Vol. 8,2007, 55

[26] Levy Y., Degani D., Seginer A., “Graphical visualization of vortical flows by means of helicity,” *AIAA Journal*, 1990, 28(8): 1347-1352.

[27] Liu C., Gao Y. S., Dong X. R. et al., "Third generation of vortex identification methods: Omega and Liutex/Rortex based systems," *Journal of Hydrodynamics*, 2019, 31(2): 205-223.

[28] Liu C., Gao Y., Tian S. et al., "Rortex-A new vortex vector definition and vorticity tensor and vector decompositions," Physics of Fluids, 2018, 30(3): 035103.

[29] Liu, C., Yan, Y., and Lu, P., "Physics of turbulence generation and sustenance in a boundary layer," Computers & Fluids, Vol. 102, 2014, pp. 353-384 .

[30] Liu, Chaoqun, et al. "Liutex and Third Generation of Vortex Identification Methods." Liutex and Its Applications in Turbulence Research, ISBN. 978-0-12-819023-4, Elsevier, 2021. https://doi.org/10.1016/B978-0-12-819023-4.00007-0

[31] Liu, Chaoqun, et al. "Short review of three generations of vortex identification methods." Liutex and Its Applications in Turbulence Research, ISBN. 978-0-12-819023-4, Elsevier, 2021. https://doi.org/10.1016/B978-0-12-819023-4.00009-4

[32] Liu, C., Wang, Y., Yang, Y., and Duan, Z., "New Omega Vortex Identification Method," Science China Physics, Mechanics & Astronomy, Vol. 59, No. 8, 2016, pp. 1-9.

[33] Liu, C., Gao, Y., Tian, S., Dong, X., "Rortex–A new vortex vector definition and vorticity tensor and vector decompositions," Physics of Fluids, 2018, 30(3): 035103.

[34] Liu, J., and Liu, C., "Modified normalized Rortex/vortex identification method," Phys. Fluids, Vol. 31 (6), 2019, 061704.

[35] Robinson S. K., "Coherent motion in the turbulent boundary layer," *Annual Review of Fluid Mechanics*, 1991, 23: 601-639.

[36] Roth M., "Automatic extraction of vortex core lines and other line-type features for scientific visualization," Doctoral Thesis, Zürich, Switzerland: ETH Zürich, 2000.

[37] Strawn R. C., Kenwright D. N., Ahmad J., "Computer visualization of vortex wake systems," *AIAA Journal*, 1999, 37(4): 511-512.

[38] Sujudi D., Haimes R., "Identification of swirling flow in 3D vector fields," AIAA Paper 95-1715, 1995.

[39] Wang, Yq., Gao, Ys., Xu, H. et al., "Liutex theoretical system and six core elements of vortex identification," J Hydrodyn 32, 197–211 (2020). https://doi.org/10.1007/s42241-020-0018-0

[40] Wang, Y., Yang, Y., Yang, G., and Liu, C., "DNS study on vortex and vorticity in late boundary layer transition," Communications in Computational Physics, Vol. 22, No. 2, 2017, pp. 441-459.

[41] Wang, Yq., Gao, Ys., Xu, H. et al. “Liutex theoretical system and six core elements of vortex identification.” J Hydrodyn 32, 197–211 (2020). https://doi.org/10.1007/s42241-020-0018-0

[42] Wang, C.et al. “On the Vortical Characteristics of Horn- Like Vortices in Stator Corner Separation Flow in an Axial Flow Pump.” Journal of Fluids Engineering, 2021, DOI:10.1115/1.4049687. https://asmedigitalcollection.asme.org/fluidsengineering/article-abstract/143/6/061201/1095493/On-the-Vortical-Characteristics-of-Horn-Like?redirectedFrom=fulltext

[43] Xu, H., Cai, Xs. & Liu, C., “Liutex (vortex) core definition and automatic identification for turbulence vortex structures,” J Hydrodyn 31, 857–863 (2019). https://doi.org/10.1007/s42241-019-0066-5

[44] Yan, Y., Chen, C., Huankun, F., and Liu, C., “DNS study on K-vortex and vortex ring formation in flow transition at Mach number 0.5,” J. Turbulence, Vol. 15, No. 1, 2014, pp. 1-21.

[45] Zhou, J., Adrian, R. J., Balachandar, S. & Kendall, T. M. “Mechanisms for generating coherent packets of hairpin vortices. ” J. Fluid Mech, 1999, 387, 353–396.

BIOGRAPHICAL INFORMATION

Dalal Almutairi was born in Riyadh, Saudi Arabia, and has grown up in Majmaah city, Saudi Arabia. She received her B.S in Mathematics from Majmaah University, Majmaah city, Saudi Arabia, in 2010. During her bachelor study, she was awarded the Outstanding Undergraduate Students from Majmaah University four times in a row in the amount of 4,000 Saudi Riyals. She earned her master's degree in Mathematics from Pittsburg State University, the USA, in December 2015. She was awarded the Outstanding Graduate Students from the Graduate School at the Pittsburg State University for achieving a perfect GPA of 4.00. After joining the Department of Mathematics at the University of Texas at Arlington as a Ph.D. student, Dalal is awarded a 2020-2021 Michael B. and Wanda G. Ray Fellowship in the amount of $1,500. Recently, she received the Dissertation Fellowship from the Graduate School at UTA for Summer 2021 for $7,000. Her research interests include Computational Fluid Dynamics (CFD) applications, applied linear algebra, and applications of PDE and ODE.